Instituto de Física Teórica
UAM-CSIC

UNIVERSIDAD AUTÓNOMA DE MADRID

FACULTAD DE CIENCIAS

DEPARTAMENTO DE FÍSICA TEÓRICA

PHD THESIS:

FAST SCRAMBLERS AND EVENT HORIZONS

Memoria de Tesis Doctoral realizada por

Javier Martínez Magán

Dirigida por:

José Luis Fernández Barbón

Investigador Científico del
Instituto de Física Teórica del
Consejo Superior de Investigaciones Científicas.

Dedicado a todas aquellas personas que
en soledad y en compañía generan espacios...
infinitos lugares donde otros, más tarde,
nos sentimos y nos movemos cada vez más libremente.

Agradecimientos

Agradezco a todas y a cada una de esas personas con las que tengo la fortuna de guardar una íntima relación.
Gracias por haberme dejado *entrar* y *permanecer*, por haber vivido el tiempo conmigo.
Os quiero mucho a todos.

Prologue

This Thesis develops recent work [1] [2] [3] [4] on the 'Fast Scrambling Conjecture' [5] [6] [7]. According to this proposal, black holes are the most efficient information scramblers in nature, with a characteristic time scale that saturates parametrically the causality bounds.

In this work we review the original motivations of this conjecture and present a number of new results, which might be considered as supporting evidence. In particular we arrive to two main ideas.

The first observation is that standard local diffusion achieves fast scrambling in spaces with hyperbolic geometry. This includes classical models such as chaotic billiards, as well as more sophisticated constructions such as random walks on expander graphs or hydrodynamic behaviour of Local Field Theories on Hyperbolic spaces.

The second observation is that the required hyperbolic structures are naturally found in the Hamiltonian formalism for standard QFT near a regular event horizon. We introduce a frame for the description of near-horizon bulk dynamics whose phase space is naturally parametrized by a quantum system on a hyperboloid. The technical specification of this frame introduces an operational definition of the notion of 'Stretched Horizon' (SH).

Finally, we use these notions to build phenomenological models for fast scrambling. In particular, the non-local dynamics of the SH can be shown to be a fast scrambler if the system is endowed with an *ultrametric* structure, a notion also found in the study of disordered systems and spin glasses.

We conclude with a set of ideas and speculations regarding the *ab initio* approach to find a proof of the conjecture in systems with high non-locality such as matrix quantum mechanics, which is the standard baseline model for a fast scrambler as suggested by holographic constructions.

The first chapter contains two parts. It begins with an introductory review to some problematic aspects of Quantum Black Holes. They will provide the specific context in which this work has been developed. The second part will deal with the origins of the so-called "Fast Scrambling Conjecture" [5] [6] [7]. It will review the three heuristic arguments leading to the conjectured time scale, namely the *no-cloning bound*, the diffusion of charged densities in the SH and the non-local, *completely connected*, dual Matrix Models of Black Holes. We show how the two first heuristic arguments have a geometrical origin, and depend solely on the *free fall* time to the SH.

The second chapter delves deeper into the geometrical aspects of this *free fall* time scale, which we explore in different types of Black holes and Black Branes. We show that Fast Scramblers must be *small*. The thermal length β of the Black Brane should exceed whatever *compact tranverse* length is characterizing the system. This is an expectable result when embedding these type of considerations in holographic frameworks. Indeed, in cases when the opposite is true, and the transverse compact directions exceed the thermal length, the *free fall* time will depend solely on the properties of a single thermal length, signalling that Fast Scrambling only occurs within a *thermal cell*, consistent with causality bounds in the dual theories. In the last part, we will show how T-duality constructions lead us to an effective Matrix Model description of this *thermal cell*.

The third chapter focuses on a search for simple examples of Fast Scramblers. At first, this time scale will be defined. Two main lines of attack will be drawn: a more fundamental type and a pragmatic one, based on diffusion. During the thesis, the main results will come from this last approach, and some justifications will be given in order to understand the connection to the first one. Using the diffusion framework, we will show how Fast Scramblers can be local under the condition that the diffusion process occurs in an effective hyperbolic geometry, or in their discrete counterparts, the so-called expander graphs. In view of these results, an application of the fundamental approach to these types of systems will be considered, leading to various insights.

The fourth chapter focus specifically on the gravitational description of Black Holes and Black Branes. The central observation will be the mapping between the near horizon physics and a thermal field theory defined on a hyperbolic geometry. In turn, the specifics of this

mapping provide us with a definition of the SH. The size of this hyperbolic space, naturally *cut-off* by the SH, will be equivalent to the flight time of a null ray as it crosses the near horizon region. With this construction in mind, we propose two models of Black Hole Fast scrambling that depend on the specific dynamics of the Hyperbolic Theory, either strongly coupled or weakly coupled. Finally, these considerations suggest a specific model of Fast Scrambling for the Planckian SH, which is of an Ultrametric type and saturates stability bounds.

We conclude the thesis by summarizing our results.

Contents

Chapter 1

Black Holes and Quantum Information

Fast scramblers find their *raison d'etre* in the quantum physics of black holes. We thus begin with an outline of the broader context of quantum black hole physics as developed in the last few decades.

1.1 Quantum Black Holes

In classical physics, black holes are absolute absorbers of matter, which in turn implies they are absolute absorbers of information. The discoveries of the 70's, prompted by the ground-breaking results of Bekenstein and Hawking [8] [9], completely altered this view. In particular, it was suggested that black holes have a finite number of degrees of freedom, signified by the finiteness of the black hole entropy:

$$S = \frac{A_H}{4G} \tag{1.1}$$

where A_H is the area of the event horizon and G is Newton's constant. Associated to this entropy, there is a natural temperature

$$T = \frac{1}{8\pi GM} \tag{1.2}$$

for a Schwarzschild black hole of mass M in four dimensions. Since the black hole radius is $R = 2GM$, one finds that the characteristic temperature is set by the size of the hole, $T \sim 1/R$, and the entropy

is the horizon volume (area) in Planck units, two statements that do generalize to arbitrary space-time dimensions.

Up to numerical constants, the Newtonian potential of a mass M at distances of order R scales as GM/R^{d-2} in $d+1$ dimensions. Therefore, the size of a black hole is parametrically related to its mass through

$$R^{d-2} \sim G\,M \tag{1.3}$$

It follows that, in any dimension, the entropy defined by the Bekenstein–Hawking formula (1.1) measures the number of minimally gapped quanta of energy $1/R$ that would account for the mass of the hole while still fitting inside:

$$S = \frac{A_H}{4G} \sim \frac{R^{d-1}}{G} \sim \frac{M}{1/R} \sim M\,R \tag{1.4}$$

These quanta are precisely the Hawking particles, emitted in the evaporation process with typical frequency $\omega \sim 1/R$. Since about one quantum is emitted every time interval of order R, the whole set of S quanta accounting for the total mass of the hole will be emitted in an evaporation time of order

$$\Gamma^{-1} \sim R\,S \tag{1.5}$$

where Γ can be interpreted as a decay width of the black hole, understood as an intermediate resonance in a scattering experiment.

A black hole is called semiclassical when $S \gg 1$. The reason for this definition is as follows. The low-energy effective field theory in the Schwarzschild metric has curvature of order $1/R^2$. Hence, quantum corrections to General Relativity (GR) on this background are of order G/R^2 or, more generally of order $\lambda = G/R^{d-1}$ in $d+1$ space-time dimensions, which serves as the expansion parameter of local effective field theory. One notices that, as a general rule in any dimensionality

$$S \sim \frac{1}{\lambda} \tag{1.6}$$

so that the semiclassical domain $\lambda \ll 1$ is equivalent to the 'large black hole' limit $S \gg 1$ and the quantum loop expansion of the effective QFT in the black hole background is an expansion in powers of $1/S$.

Large-entropy black holes can be thought of as extremely narrow resonances, since

$$\frac{\Gamma}{M} \sim \frac{1}{S^2} \ll 1 \tag{1.7}$$

so that, for time scales much shorter than the evaporation time

$$t_{ev} \sim \Gamma^{-1} \sim R\,S \tag{1.8}$$

we can neglect Γ and regard them as stable states diagonalizing an effective Hamiltonian with eigenvalues given by the spectrum of black hole masses. The density of states of such effective Hamiltonian is however rather exotic, since the dimension of the effective Hilbert space is

$$\mathrm{d}im\,\mathcal{H}_{eff} \sim \exp(S) \sim \exp(G^{\frac{1}{d-2}} M^{\frac{d-1}{d-2}}) \tag{1.9}$$

The very strong growth at high energies, making the entropy function concave, is responsible from the thermodynamical instability of black holes (negative specific heat) and more generally complicates the task of identifying a model for the effective Hamiltonian of a quantum black hole. In fact, such a radical growth of states with energy is incompatible with local dynamics in time, as shown in [10]. This suggests that we should somehow cut-off the growth of (1.9) in order to find more standard descriptions.

One possibility is to enclose the system in a spatial box of size L. It is easy to see that in such a finite system a small amount of Hawking radiation can come to equilibrium with a sufficiently large black hole (cf. for example [11]), rendering the state stable. Its mass should then be a true eigenvalue of a Hermitian Hamiltonian, still with the exotic density of states (1.9), but now cutoff at a maximal energy corresponding to the largest black hole fitting inside the box, i.e. one with Schwarzschild radius $R \sim L$.

The simple arguments advanced so far have a startling consequence. The states with largest energy which can be said to be localized within a region of size L are typically black holes with a size of order L. On the other hand, their entropy (log of the density of states) scales like the volume of the bounding region. Therefore, we conclude that a hypothetical description with local degrees of freedom

on the boundary of the region has enough states to account for any state fitting in the interior. One possible interpretation of this fact would be to admit that local QFT is a vastly redundant description of the full quantum physics within the size L. In particular, once the states are massive enough to look like black holes, a description based on boundary degrees of freedom becomes more natural. Since high-energy states (black holes) have vastly more entropy than lower energy particle-like QFT states, we may entertain the possibility that the boundary variables are the more fundamental ones, with QFT arising as an effective description for sufficiently 'dilute' states not containing black holes.

The previous paragraph is the statement of the famous Holographic Principle [12,13]. In order to make progress we would need to guess the Hamiltonian written in 'boundary variables'. This looks rather like an impossible task, since the density of states was pointed out to be completely exotic, not featuring in 'textbooks', i.e. qualitatively different from any other Hamiltonian previously encountered in nature.

This *impasse* was jumped over by Maldacena with his famous discovery of the AdS/CFT correspondence [14, 15]. From the point of view of the present discussion, the AdS/CFT correspondence offers an 'ultraviolet completion' of the boxed black hole system, by the use of a clever type of box: Anti de Sitter space-time.

It is well known that the maximally symmetric space-time of negative curvature, denoted AdS_{d+1}, acts as a soft box with a confining gravitational potential of a simple harmonic form at large distances:

$$V_{eff}(r) \sim \left(\frac{r}{L}\right)^2 \tag{1.10}$$

for $r \gg L$ and L interpreted here as the radius of curvature of AdS. [1] Hence, we have the physics of a box, but black holes with $R \gg L$ are still possible, except that they behave very differently from Schwarzschild black holes with $R < L$. In particular, their entropy is a convex function of the energy, ensuring positive specific heat:

$$S_{R\gg L} \sim S_*^{1/d}(ML)^{\frac{d-1}{d}} \tag{1.11}$$

[1] The radial coordinate r is defined so that $r = constant$ spheres have volume $|\mathbf{S}^{d-1}|r^{d-1}$.

with $S_* = L^{d-1}/G$ the crossover entropy at the threshold mass separating small and large black holes, given by

$$M_* \sim \frac{L^{d-2}}{G} \tag{1.12}$$

The crucial insight is to recognize (1.11) as the ordinary entropy of a massless QFT (more precisely a CFT) in d space-time dimensions and with S_* particle degrees of freedom (in spin, color, flavor, etc). Thus we can guess that the complete quantum gravitational theory in AdS_{d+1} can be captured at the quantum level by a CFT in one dimension less, defined in a spherical box of size L, but with no dynamical gravity.

This guess is the substance of the celebrated AdS/CFT correspondence. Additional evidence comes from the fact that the asymptotic isometry group of AdS_{d+1} is $SO(2,d)$, which matches the conformal group in d space-time dimensions, as well as a plethora of more detailed tests in more specific versions of the correspondence with larger (super)symmetry structures.

The AdS/CFT correspondence implies that large AdS black holes, with $R \gg L$, are equivalent to typical high energy states in the finite-volume CFT, like for instance high-temperature quark-gluon plasmas. Such systems have canonical thermodynamics with entropy

$$S \sim S_* \, (L\,T)^{d-1} \tag{1.13}$$

where we see how S_* acquires the interpretation of particle-like degrees of freedom. Small Schwarzschild-like black holes, with $R \ll L$, are not so easy to identify as states in the CFT, since their very existence relies on the $S_* \to \infty$ limit. At any rate, the AdS/CFT correspondence provides an embedding of all the classic problems of quantum black hole physics in terms of a comparatively controlled system: a CFT without gravity in the limit of parametrically large number of degrees of freedom $S_* \gg 1$.

1.1.1 Crisis... What Crisis?

The fully quantum mechanical description of black holes implied by the holographic ideas is fundamentally non-local in the original space-time. A tension between unitarity and locality was evident from the

very early results by Hawking and his famous 'information paradox' [**?**].

At a technical level, the derivation of black hole radiance relies on the assumption that the QFT state of low-energy fields in the near-horizon region is well approximated by the vacuum. This is required by the Equivalence Principle (EP), since such a state can be measured by a small infalling observer entering the black hole. It follows that, to a good approximation, the Hawking quanta remain maximally entangled with degrees of freedom left behind in the hole, and thus the entropy of the Hawking quanta measured at infinity is very close to maximal (i.e. thermal) for all quanta emitted while the black hole is still semiclassical (i.e. satisfying $S \gg 1$). This condition is only violated when $S \sim 1$, which corresponds to a Planck-sized black hole of the order of the Planck mass. Hawking's information paradox is the statement that unitarity must be violated because quantum purity of the Hawking radiation cannot be restored by the final Planckian burst of particles, accounting only for a tiny fraction $M_{\mathrm{P}lanck} \ll M$ of the initial mass.

This paradox is a clash between the two founding principles of XX century physics: unitarity and locality. Despite the original proposal by Hawking himself that unitarity was the culprit, the opposite option has been gathering consensus in the last couple of decades. In particular, holographic ideas point very definitely towards the breakdown of standard locality. The success of the EP is tied to the success of local QFT which, as argued above, is an expansion in powers of $1/S$ in the black-hole spacetime. Therefore, salvaging the EP requires the locality violations to be invisible to all orders in the $1/S$ expansion.

We can estimate the size of the required locality violations by a kind of 'fluctuation-dissipation' argument. Let $\mathcal{O}_{\mathrm{in}}$ and $\mathcal{O}_{out}$ local observables associated to 'infalling' and 'outgoing' degrees of freedom, with spacelike separation in the smooth black hole metric, so that they commute to all orders in the $1/S$ expansion. We can guess that the size of the commutator in the black hole state can be estimated by the size of out-out correlations at the time where information must be returned, i.e. the evaporation time:

$$\langle [\mathcal{O}_{\mathrm{in}}, \mathcal{O}_{out}] \rangle_{\mathrm{b}h} \sim \langle \mathcal{O}_{out}(0)\, \mathcal{O}_{out}(t_{ev}) \rangle \tag{1.14}$$

The right hand side decreases with time as $\exp(-t/R)$, according to

the classic no-hair theorem, so that its value at $t = t_{ev} = R\,S$ is of order $e^{-S} = e^{-1/\lambda}$. The required locality violation is then non-perturbative in the expansion parameter of low-energy effective QFT, explaining why Hawking's argument did not see the restoration of unitarity. More abstractly, any low energy QFT treatment is an expansion around $S = \infty$, but the information is never returned in the $S = \infty$ case, the evaporation time being infinite. On the other hand, the quasinormal behavior of quantum correlations

$$\langle \mathcal{O}_{out}(0)\, \mathcal{O}_{out}(t) \rangle \sim e^{-t/R} \tag{1.15}$$

can only be exact in the strict $S = \infty$ limit. At finite S, the spacing of energy levels of the black hole Hamiltonian is of order $T\, e^{-S}$, so that any correlation function of type (1.15) suffers from 'quantum noise' at very long times, of the order of the Heisenberg time

$$t_{\rm H} \sim R\, e^{S} \tag{1.16}$$

setting the scale of $\mathcal{O}(1)$ Poincaré recurrences in (1.15). Since the tiny energy spacings, of order e^{-S} are invisible in low-energy QFT (being a theory only defined in powers of $1/S$), any local QFT argument treats the spectrum of black hole states as continuous.

An *ab initio* fix of this problem is to rely completely on holographic variables, such as the CFT in the case of AdS black holes. This has the high cost of sacrificing *completely* the locality of the bulk spacetime. More modestly, a semi-phenomenological fix to this problem is the introduction of the 'stretched horizon' (SH). Physically, the origin of the 'disease of the continuous spectrum' is the infinite redshift at the black hole horizon. This can be fixed provisionally by imposing a cutoff at a timelike surface which sits one Planck unit above the horizon. This surrogate of the horizon, equipped with some effective Hamiltonian, is the SH. The use of stretched horizons goes back to the so-called 'membrane paradigm' [16–18], an effective Newtonian model for the interactions of realistic black holes with various astrophysical surroundings.

We can view the SH model as a parametrization of finite S effects, while keeping the broad formalism of local QFT in the vicinity of the horizon. Roughly, we ascribe the non-local effects of order e^{-S} to the physics of this quantum system extended over the horizon with

a density of degrees of freedom of order one bit per Planck area. Ultimately, the notion of the SH together with its effective Hamiltonian must be derived from the putative holographic description. Provisionally, physically motivated models like the SH can be used to explore the physics of the problem.

Viewed from the point of view of the $\mathcal{O}_{out}$ operator algebra, the SH is a highly chaotic system which quickly thermalizes any quantum state that it absorbs, and the energy is released back in the form of Hawking radiation. This picture puts the black hole on the same footing as any other complex highly excited system which *processes* information as a randomizer.

There are two main differences between an ordinary thermal system and the black hole. The first and more important is that such a picture only applies to the $\mathcal{O}_{out}$ operator algebra associated to S-matrix type questions or, more colloquially, to 'external observer measurements'. Infalling observers, carrying the $\mathcal{O}_{in}$ operator algebra, see no SH whatsoever. In fact they just measure the local vacuum state of the low energy QFT, in accordance with the EP. This dichotomy of Bohr's type has been argued by Susskind to be exactly that: a case of quantum complementarity between two sets of non-commuting operators. This idea, dubbed 'the principle of black hole complementarity' [19], is the most important open question in the study of quantum black holes. Exactly how to implement the unitarity transformation between the *out* and the *in* operator algebras remains a subject of intense debate [2]

The second difference between black holes and generic randomizers is the occurrence of new 'short' dynamical time scales associated to the thermalization process, which are characteristic of the black hole dynamics. They are the subject of the next section and indeed of the main body of this thesis.

1.2 Why Fast Scramblers?

The conceptual scenario laid down in the previous section suggests that, viewed in the context of information theory, black holes

[2]Recently, the discussion of *firewalls* [20] has elevated the tone of the discussion, putting into question the very validity of the complementarity principle.

are just efficient thermalization systems, characterized by one basic time scale, T^{-1} the Hawking temperature, while a number of detailed physical properties depend on the existence of a parametrically small (but finite) number $\lambda = 1/S$ which controls the accuracy of the semiclassical picture. In particular we have two additional *very long* time scales: the black hole lifetime in Minkowski space:

$$t_{ev} \sim T^{-1}\, S \tag{1.17}$$

and the Heisenberg time scale (setting the Poincaré recurrences) for a black hole in a commensurate box (or AdS for that matter):

$$t_{\rm rec} \sim T^{-1}\, e^{S} \tag{1.18}$$

In this section we lay down a number of arguments suggesting that a third time scale is present, associated to the global scrambling of information, and having a logarithmic dependence on the entropy. This time scale is associated to the universal presence of a near-horizon region of Rindler type, associated to any SH, to the extent that one may naturally view the SH and its associated Rindler region as a dynamical unity.

1.2.1 The Conjecture

From this information theoretical point of view, black holes may be regarded as *efficient* randomizers. A phenomenological description in terms of a SH, with a highly chaotic Hamiltonian, embodies this assumption. An interesting question in this respect is whether some special dynamics, peculiar of black holes, must be postulated, or we can regard the information processing by a black hole just like the information processing in a hot gas.

The holographic description of black holes as plasma states in QFT's seems to indicate that no exotic thermalization properties are to be expected. On the other hand, large semiclassical black holes arise precisely at very strong coupling and in the large N limit in the field-theory side, and thus standard QFT intuition must be reexamined. In fact, there are reasons to believe that black holes have peculiar thermalization properties, in the sense that they scramble information essentially as fast as it is possible, compatible with causality. This was

proposed in [5,6], and it comes under the name of The Fast Scrambling Conjecture. The *scrambling time* for black holes was conjectured to be

$$\tau_s \sim T^{-1} \log(S) \,, \tag{1.19}$$

with T the Hawking temperature and S the black hole entropy.

To have a feeling of how fast this is, one may take an straightforward diffusion argument. In systems with local degrees of freedom and local interactions the scrambling of information can often be assimilated to a diffusion process. In this case, if the diffusion takes place in flat space, we can say that locally coded information 'random-walks' around the system, covering a volume L^d in a time proportional to L^2. For 'normal' states, with extensive entropy, $S \propto L^d$, we find *scrambling times* proportional to $S^{2/d}$, measured in units of some typical time scale characterizing the state, such as the inverse temperature $\beta = T^{-1}$ in relativistic systems [3].

Therefore, roughly, 1.19 corresponds to the local scrambling for a system with infinite spatial dimension, $d \to \infty$. It is very interesting to elevate this estimate to the rank of fundamental law of nature, and regard black holes as the fastest possible scramblers [6].

The fast scrambling rate of black holes can be argued in a number of ways. It turns out that τ_s is the time scale that saturates the no-cloning bound in black holes, i.e. it is a measure of the minimum time for information retrieval in the Hawking radiation (cf. [5,6]). The same time scale can be identified in a kinematical effect characteristic of the 'membrane paradigm' [16–18], where a conserved charge distribution on the stretched horizon, induced by the motion of external charges, undergoes non-relativistic Ohmic diffusion with respect to the Schwarzschild time variable. It follows that this induced charge spreads exponentially fast, filling a given area of horizon in a time which scales logarithmically with this area. Finally, from the point of view of hypothetical holographic duals of the black hole, both Matrix

[3] We will argue the diffusion model for computing the scrambling in the third chapter. At the same time we will be more rigorous in describing diffusion and Random Walks in the fourth chapter. For the time being just notice that there is also another bound, given by the time a perturbation takes to cross the system in the vacuum state of the theory. This gives a *causality bound* for the scrambling time of the order $\mathcal{O}(S^{1/d})$ for flat space models

Theory [21] and AdS/CFT [14] suggest the consideration of $N \times N$ matrix models with $S \sim N^2$ degrees of freedom. The non-local character of the interactions of matrix elements in 'index space' suggests that, precisely for these systems, we may get the maximal possible scrambling rate.

We develop more in these three constructions in what follows.

1.2.2 The no-cloning bound

We begin describing the no-cloning argument by noticing Figure 1.1, which illustrates the fact that the edge of the near-horizon region, given by the line $X^+X^- = -R_s^2$, is symmetric to the singularity locus, $X^+X^- = R_s^2$, by a null reflection through the horizon. This fact will be essential for our later observations. The points Q and Q' are also symmetric and separated a proper distance of order ℓ_p from the horizon.

If a Q-bit falls into the black hole from P to Q while it is cloned at the horizon and returns within the Hawking radiation at P', a local verification of the cloning could occur inside the black hole if Q and P' can have a common point S in their future. Notice that the points P and P' are set at height R_s because the cloned Q-bit must be efficiently detected while it is emitted with wavelength of $\mathcal{O}(R_s)$. This situation being incompatible with the linear evolution of quantum mechanical states, it must be that such a local meeting of the two copies is prevented by the occurrence of the singularity. In this way we obtain a lower bound on the time delay between the two departures of the infalling Q-bit from P and P'.

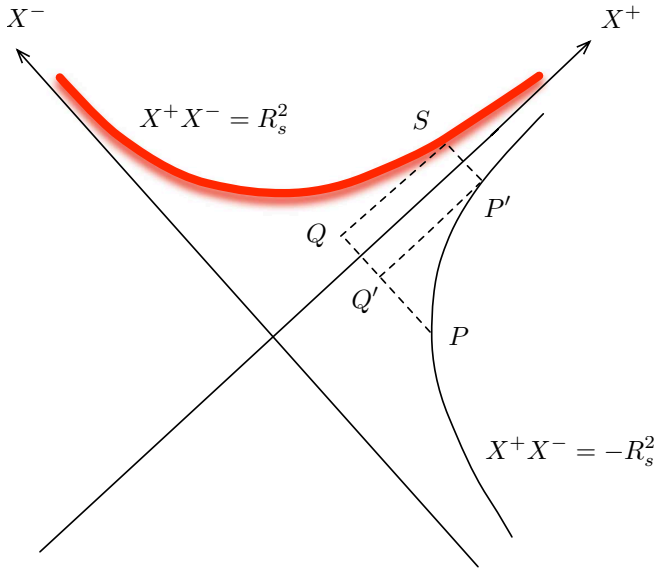

Figure 1.1: Diagram showing that the Schwarzschild time between P and P' equals the reflection time of a photon from the stretched horizon, i.e. the piecewise-null trajectory $P\,Q' \cup Q'\,P'$, where Q and Q' lie respectively at the inner and outer edges of the stretched horizon, i.e. on the hypersurfaces $X^+X^- = \pm\ell^2$.

We compute this delay using the standard map between Schwarzschild time and Kruskal coordinates, $X^\pm \sim R_s \exp(\pm t/2R_s)$. Since Q' sits at the edge of the stretched horizon we have $X^+_{Q'}X^-_{Q'} = -\ell_p^2$. Furthermore, $X^+_{P'}X^-_{P'} = -R_s^2$ and, by the reflection conditions $X^-_S = X^-_Q = -X^-_{P'} = -X^-_{Q'}$, we find

$$\Delta t_{min} \sim 2R_s \log\left(\frac{X^+_{P'}}{X^+_P}\right) = 2R_s \log\left(\frac{R_s^2}{\ell_p^2}\right) . \tag{1.20}$$

Noting that the entropy $S = \frac{A}{4G} \sim (R_s/\ell_p)^2$ we find, up to $\mathcal{O}(1)$ coefficients and neglecting $\mathcal{O}(R_s)$ additive contributions,

$$\Delta t_{min} \sim \tau_* = R_s \log(S) . \tag{1.21}$$

Since ℓ_p enters logarithmically, this time scale is very robust in order of magnitude. For example, the same result is obtained with the much less conservative criterion that $X^-_Q > M^{-1}$, with M the

mass of the black hole, so that the infalling Q-bit is not heavier than the original black hole.

We point out, for later convenience, that in this construction it is clear that the time-delay scale, τ_*, is equal to the 'reflection time' from the SH or, in order of magnitude, a minimal free-fall time to the SH across the Rindler region. In the last chapter we will compute this quantity for generic black holes. We shall denote this kinematical time scale as the 'optical depth', in relation with the size of the *optical metric*, to be described later on as well. These simple observations will be central in all our scrambling models for Black Holes.

On the other hand, the actual relevance of these arguments for the issue of information retrieval is not clear. As was pointed out in [1], and carefully developed in [22], the complete *decoding* of the information contained in a single Q-bit may require time scales in excess of $\mathcal{O}(R_s\, e^S)$, the Heisenberg time of the system.

1.2.3 Classical diffusion at the Streched Horizon

A second argument introducing the time scale $\tau_* = R_s \log(S)$ uses the dynamics of induced charge densities on the stretched horizon according to the membrane paradigm [6, 16–18]. Generically, charges densities are just given by the normal component of the Electric field, solution to the classical equations of motion, at the given surface. We review here the simple and clear approach exposed in [18]. We consider a rest charge at position z_c in Minkowski coordinates, with the electric field given by

$$E_z = \frac{e(z - z_c)}{[(z - z_c)^2 + x_\perp^2]^{\frac{3}{2}}} \ . \tag{1.22}$$

The purpose is to study physical quantities at the SH in the Rindler frame, with metric

$$ds^2 = -\rho^2 d\omega^2 + d\rho^2 + dx_\perp^2 \ . \tag{1.23}$$

The SH is sited at $\rho_{SH} = \ell_p$. Computing the normal component of the Electric Field at this surface $E_{\rho_{SH}}$ is a simple exercise, because the Rindler wedge is related to the more common Minkowski one by a boost along the z axis. In particular, the component along the boost direction is invariant

$$E_\rho = E_z = \frac{e(z-z_c)}{[(z-z_c)^2+x_\perp^2]^{\frac{3}{2}}} = \frac{e(\rho\cosh\omega - z_c)}{[(\rho\cosh\omega - z_c)^2+x_\perp^2]^{\frac{3}{2}}} \ . \quad (1.24)$$

The surface charge density is defined as

$$\sigma = \frac{1}{4\pi\rho}E_\rho|_{\rho_{SH}} = \frac{e}{4\pi\ell_p}\frac{\ell_p\cosh\omega - z_c}{[(\ell_p\cosh\omega - z_c)^2+x_\perp^2]^{\frac{3}{2}}} \ , \quad (1.25)$$

which, in the limit $\omega \gg 1$, is well approximated by

$$\sigma = \frac{1}{4\pi\rho}E_\rho|_{\rho_{SH}} = \frac{e}{4\pi\ell_p}\frac{\ell_p e^\omega}{[(\ell_p e^\omega)^2+x_\perp^2]^{\frac{3}{2}}} \ , \quad (1.26)$$

giving an exponential spreading of the surface charge density along the transverse directions

$$x_\perp \sim \ell_p e^\omega \ . \quad (1.27)$$

In the case of a Schwarzschild Black Holes 1.27 gives the conjectured time scale in order of magnitude.

Another view of these dynamics, which connects with the free fall time observation of the no-cloning argument, is that spacetime variations of these surface densities should not violate local causality. The fastest possible variations of such electromagnetic fields are induced by letting a moving source charge above the horizon approach the speed of light. This leads naturally to the time scale τ_*, since that is the characteristic time for the source charge to cross the near horizon region and hit the SH, as we have just mention when describing the no-cloning argument.

Indeed one may think that an exponentially fast spread, as measured in asymptotic time, is incompatible with causality. A simple argument from [13] shows that such a behavior is precisely *s*aturating the causality bound, rather than contradicting it. Let us define the SH in locally flat coordinates $(X^+, X^-, X_\perp)$ as the Rindler surface

$$X^+X^- \equiv -(X^0)^2 + Z^2 = \ell_p^2 \ . \quad (1.28)$$

The future light-cone bounding causal events originating at a point of coordinates $(X^0 = 0, X_\perp = 0, Z = \ell_p)$ on the SH is given by

$$-(X^0)^2+(Z-\updownarrow_p)^2+X_\perp^2=0\ , \tag{1.29}$$

which intersects the SH itself along the hypersurface

$$X_\perp^2=2\ell_p(Z-\ell_p)\longrightarrow 2\ell_p^2\,e^{t/2R_s}\ ,\ , \tag{1.30}$$

where we have inserted the long-time asymptotics of $Z\sim X^+-X^-$, with respect to the asymptotic Schwarzschild time variable, showing the exponential rate which fills an area of order $X_\perp^2\sim R_s^2$ in a time of order τ_*.

Notice that the light rays between two points on the stretched horizon do not propagate confined to the stretched horizon, but actually go *above* it through the bulk of the Rindler region.

Another equivalent face of these considerations, which will be crucial in what follows, is the study of this peculiar causality constraint in the so-called *optical metric*, obtained by rescaling the physical metric in such a way that the static redshift disappears, i.e. for 1.23 we have

$$\widetilde{ds}^{\,2}=-dt^2+\frac{d\rho^2+d\vec{x}^{\,2}}{\rho^2}\ ,\ , \tag{1.31}$$

which describes the direct product of the time line with a hyperbolic space. Being conformally related, the metrics1.23 and 1.31 share the same local causality structure. In particular, null paths connecting two points at the SH surface correspond to geodesic hyperbolic arcs in the $\mathbf{H}^{d+1}$ space, cut-off at ρ_{SH}. The resulting time of flight across a $\vec{x}$-coordinate domain of magnitude $2L$ is

$$t_L=2\log(L/\ell_p)=2z_L\ ,\ , \tag{1.32}$$

where we have defined the tortoise coordinate
$z=\log(\rho/\ell_p)$
normalized so that $z_{SH}=0$ at the stretched horizon. Equation 1.32 shows that the fastest causal connection between two points separated by an amount of order L in the SH scales only logarithmically with L. This contrasts with the causal time for any transport *within* the SH which, if taken in isolation, would be proportional to L, or even $\mathcal{O}(L^2)$ if the usual diffusion processes are assumed.

We then observe that the root of these two first heuristic arguments, the no cloning bound and the charge spreading, is the same,

being the specific and peculiar nature of the free fall time of null geodesics in the near horizon region. At the same time these geodesics and, therefore, the causal structure of the SH, can be naturally described in the *optical frame*, in which the background geometry is the product of the time line times an Hyperbolic space.

Going back to *scrambling* considerations, these arguments leave us in a quandary regarding the interpretation of τ_* as a scrambling time. Since any process measured by scales of order τ_* is saturating causality in order of magnitude, this means that the purported scrambling must be not only fast but in fact as fast as it can be. Hence the suggestion that fast scramblers cannot behave like standard diffusion at all: a fast scrambler must work at *ballistic* speed.

1.2.4 Quantum Circuits and Matrix Models

The last input for the justification of the conjecture is coming from results in Quantum Information Theory [5]. In particular, in [23], it is shown that such rates are attainable within the circuit scheme of quantum computation.

The actual circuits considered in that work are as non-local as they can be. The construction can be vaguely explained by asserting that at each time step $N/2$ random pairs of Q-bits are chosen out of the N total Q-bits conforming *the circuit* or, in more physical words, conforming *the physical system*, and a random Unitary transformation in the space of two Q-bits [4] is applied to each pair. This then furnish a, unitary and discrete, time evolution for the system.

What is shown in Ref. [**?**] is that, indeed, with this procedure, after $\mathcal{O}(\log(N))$ steps have elapsed, the resulting state is almost undistinguishable from a random state taken from the Haar ensemble, which in turn is just the uniform distribution in the full Hilbert space. More precisely, after those number of steps, the resulting state is a random state taken from a *unitary two design*. These *unitary p-designs* are probability distributions over quantum states, whose averages give equal results to those obtained from the Haar ensemble, whenever the polynomial function which is studied is of degree p or less.

[4] This is a 4×4 Unitary Random Matrix, a matrix taken from the unitary Circular ensemble of 4×4 matrices

Although this is naively a very awkward and non-physical model it has indeed some relevance for Black Holes. The point here is that the existing holographic descriptions of black holes which are well defined do involve matrix models, through the gauge/gravity correspondence. In turn, matrix models are examples of systems with few-body interactions in index space, such as the standard four-point interaction potential for a $N \times N$ Hermitian matrix model:

$$\mathrm{T}r\, M^4 = \sum_{ijkln=1}^{N} M_{ij} M_{kl} M_{ln} M_{ni} \tag{1.33}$$

which are completely non-local, with a structure resembling the previously mentioned quantum circuits.

To be sure, the type of matrix models arising in the context of the gauge/gravity correspondence come equipped with a gauge symmetry, so that states must be singlets under the action of the $SU(N)$ group. However, the black hole states are associated to the part of the spectrum with entropy of order N^2, which becomes separated from the low-lying states by a large-N phase transition. For energies above the critical one, $E_c \sim N^2$ one expects that the singlet constraint plays no important dynamical role and one can approximate the dynamics by that of 'colored' degrees of freedom, i.e. the matrix entries M_{ij} or 'gluons'.

Indeed, one even may have the intuition that these models *scramble* information in one step. Initially localized information seems naively to explore the whole set of degrees of freedom in one step, if every degree of freedom is connected with every other. This would be violating the Fast Scrambling Conjecture, and would potentially furnish another problematic issue to AdS/CFT correspondence, since we have just seen, in the past two sections, how to obtain a lower causality bound for this time scale in the bulk description of Black Holes. This bulk causality bound is of $\mathcal{O}(\tau_*) \gg \mathcal{O}(1)$, and it is a time scale that should appear in the dual descriptions. We will speculate about these interesting issues in the last chapter.

Chapter 2

Fast Scramblers must be *Small*

Motivated by the observation that the free fall time through the near horizon region until the SH is of the same order of the conjectured scrambling time scale in the Schwarzschild Black Hole, we proceed to study this quantity in several Black Hole metrics, with different tranverse geometries and warped factors.

We begin with the simplest examples of Black Branes, without compact factors and a near horizon region typical of an AdS/CFT construction. The result is that the free fall time will not be related to the full entropy, but rather to the effective number of degrees of freedom of a single thermal cell in the dual theory. This result signals the intuition that Fast Scrambling just occurs within the thermal cell, and outside of it generic slow diffusion will take place, as was first suggested in [6]. Then we go on to more general cases, with D-brane geometries possessing compact factors in the bulk as well as in the world volume. The same result remains unchanged under this generalizations, but new insights appear. When the compact factors in the world volume are smaller than the thermal length, the entropy appearing in the free fall time expression is the full entropy of the D-brane system.

Given these two qualitatively distinct cases, we go and look for phase transitions interpolating between the two phases, and verify that the two laws show a smooth crossover. Moreover, within this construction, by the use of T-duality we are able to derive the effective

theory of a single thermal cell, which is given by Matrix Quantum Mechanics, the model described in [21].

One could argue that these infalling times are peculiar of massless particles. In the last section we consider other type of observables, like D-branes, and show that the results remain the same.

2.1 Black branes

We begin with geometries suited for Holographic descriptions without internal dimensions. The main purpose of this exercise is to express the result in terms of dual QFT variables in a situation where the AdS/CFT lore may be applied.

Consider a general $(d+2)$-dimensional background, $\mathbf{X}^{d+2}$, which may admit a holographic interpretation in terms of a $(d+1)$-dimensional field theory at finite temperature:

$$ds^2_{\mathbf{X}} = F(\rho)\left(-h(\rho)dt^2 + d\ell^2\right) + \frac{d\rho^2}{h(\rho)}\,, \tag{2.1}$$

where ρ is the holographic radial coordinate, parametrizing the UV regime at large ρ and the IR regime at small ρ. If the model has the luxury of being defined as a perturbation of a well-defined UV fixed point, the warp factor has the asymptotic behavior $F(\rho) \to \exp(2\rho/R_\infty)$ as $\rho \to \infty$, with R_∞ the asymptotic AdS radius of curvature. The metric of the dual QFT is defined as the asymptotic induced metric after removing the $F(\rho)$ warp factor, i.e.

$$ds^2_{\mathrm{Q}FT} = -dt^2 + d\ell^2\,, \tag{2.2}$$

where ℓ parametrizes the d-dimensional spatial manifold on which the QFT is defined. The function $h(\rho)$ models thermal effects, having a simple zero at the horizon, $h(\rho_0) = 0$, and approaching unity at large values of ρ, far from the horizon. The near-horizon, or Rindler region, reaches out to radii of order ρ_β, defined by $h(\rho_\beta) \sim 1$. In the linear approximation we have $h(\rho_\beta) \sim h_0'(\rho_\beta - \rho_0) \sim 1$, which gives an order-of-magnitude estimate for ρ_β. The Hawking temperature is given by

$$T = \frac{h_0'}{4\pi}\sqrt{F_0}\,, \tag{2.3}$$

where $F_0 \equiv F(\rho_0)$.

For future convenience we change the radial variable to the Regge-Wheeler coordinate, z defined by

$$dz = -\frac{d\rho}{h(\rho)\sqrt{F(\rho)}} \ , \tag{2.4}$$

where the minus sign is meant to indicate that z grows 'inwards'. The metric in this frame reads

$$ds^2_{\mathbf{X}} = F(z)h(z)\left(-dt^2 + dz^2\right) + F(z)\, d\ell^2 \ , \tag{2.5}$$

We proceed now to compute the flight time for a massless particle to go through the near horizon region and hit the Streched Horizon. This surface is settled at Planckian distance from the true horizon, at coordinate ρ_* defined by

$$\ell_{\rm P} = \int_{\rho_0}^{\rho_*} \frac{d\rho}{\sqrt{h(\rho)}} \sim \sqrt{\frac{\rho_* - \rho_0}{h_0'}} \ . \tag{2.6}$$

Using $h_* = h(\rho_*) \approx h_0'(\rho_* - \rho_0)$ we find the relation

$$\beta\sqrt{F_0 h_*} \sim \ell_{\rm P} \ , \tag{2.7}$$

which expresses the fact that the local blue-shifted temperature, proportional to $(F(z)h(z))^{-1/2}$, grows from $\mathcal{O}(T)$ at the edge of the Rindler region, to Planckian order $\mathcal{O}(m_{\rm P})$ at the stretched horizon.

Within this setup the free fall time takes the following form

$$\tau_* \sim z_* - z_\beta \sim \beta\, \log\left(\frac{\rho_\beta - \rho_0}{\rho_* - \rho_0}\right) \sim -\beta\, \log(h_0'\, \ell_{\rm P}) \sim \beta\, \log\left(\frac{\sqrt{F_0}}{T\, \ell_{\rm P}}\right) \ , \tag{2.8}$$

where we have neglected numerical factors of $\mathcal{O}(1)$.

In order to translate (2.8) into dual QFT variables, we compute the entropy, or horizon volume in Planck units:

$$S \sim \frac{1}{\ell_{\rm P}^d} \int d^d\ell \left(\sqrt{F_0}\right)^d \sim V \left(\frac{\sqrt{F_0}}{\ell_{\rm P}}\right)^d \ , \tag{2.9}$$

with $V = \int d^d\ell$ the volume in the QFT metric. With these conventions, the entropy in a QFT volume of one thermal length, $V_{cell} \sim \beta^d$,

is given by $S_{cell} = S/n_{cell} \sim (T\ell_{\rm P}/\sqrt{F_0})^{-d}$, where $n_{cell} = VT^d$ is the number of 'thermal cells'. Returning now to (2.8), we find, up to $\mathcal{O}(1)$ numerical coefficients, the following expression in dual QFT variables

$$\tau_* \sim \beta \, \log\left(\frac{S}{n_{cell}}\right) = \beta \, \log\left(S_{cell}\right) , \tag{2.10}$$

The entropy per thermal cell, S_{cell}, estimates the number of microscopic QFT degrees of freedom participating on a thermal state at temperature T, and supported on length scales of order β, so that we may use the notation $S_{cell} = N_{eff}(T)$. For a conformal field theory N_{eff} is asymptotically independent of the temperature and proportional to the central charge, of order $N_{eff} \sim N^2$ for CFTs based on Yang–Mills theories. For non-conformal theories it gives a sort of 'running' central charge with non-trivial scale dependence. A good example is provided by the gravity duals of the Dp-brane theories with $p < 5$, where

$$N_{eff}(T) = N^2 \, (\lambda_p \, T^{p-3} \,)^{\frac{p-3}{5-p}} , \tag{2.11}$$

with λ_p the dimension-full 't Hooft coupling of the (p+1)-dimensional Yang–Mills theory [24]. This running central charge also controls other observables related to counting of degrees of freedom, such as the entanglement entropy computed in the gravity prescription [25–27], (see [28] for such a discussion).

Just as a summary, we have shown a nontrivial relation between the free fall time to the Streched Horizon and the entropy contained in a thermal cell of the putative dual Field theory living at spatial infinity 2.10. As was commented before, this points to the intuition that Fast Scrambling should be confined to one thermal cell in the Dual Field theory, whereas outside of it common slow diffusive phenomena should take place, consistently with causality in the QFT.

2.2 Internal dimensions

In this section we look more carefully at the effects of finite horizon size in these geometrical results concerning the near horizon region and the free fall time. In particular, we consider finite-size effects in the bulk geometry, both in internal dimensions and in the geometrical

data of the dual CFT. As a concrete example, we will examine how the free fall time depends on the size of the hypothetical dual model, for the standard case of a thermal sate in maximally supersymmetric Yang–Mills theory on a toroidal box $\mathbf{T}^d$.

First let us consider compact factors in the bulk. Refinements of the AdS/CFT correspondence often involve the discussion of these compact factors spaces. In this case, the question arises as to what definition of the Planck length must be used in the two places where it appears, namely in the location of the stretched horizon and in the normalization of the entropy. We may use either the $(d+2)$-dimensional definition, or the $(d+k+2)$-dimensional definition in a background with a compact k-dimensional factor. A natural criterion would demand that we 'integrate out' the extra compact factors when their local size at the near-horizon region is smaller than the local red-shifted inverse-temperature. On the other hand, at temperatures large enough to 'see' the extra compact cycles we should use the higher-dimensional picture (see [29] [30] [31] for an 'extensive' use of this criterion in related contexts .)

A large class of holographic backgrounds can be parametrized as 'warped products' of AdS with a compact manifold of the same overall (but positive) curvature. To be more precise, consider Einstein-frame metrics parametrized in the form

$$ds^2 = \frac{r^2}{b(r)^2}\left(-h(r)dt^2 + d\ell_d^2\right) + \frac{b(r)^2}{r^2}\frac{dr^2}{h(r)} + b(r)^2\, dy_k^2\,, \qquad (2.12)$$

where $b(r)$ is a function characterizing the overall curvature, or order $1/b(r)^2$ at radius r. The coordinates y_k parametrize a k-dimensional compact factor $\mathbf{K}_k$ of $\mathcal{O}(1)$ curvature, warped by the profile function $b(r)$. The function $h(r)$ is again the thermal factor, admitting a near-horizon parametrization $h(r) \sim (r-r_0)/r_0$ in order of magnitude, so that the Hawking temperature reads $T \sim r_0/b_0^2$, with $b_0 \equiv b(r_0)$. More generally, we have an approximate UV/IR relation for the energies measured with respect to the t variable, $E(r) \sim r/b(r)^2$, as corresponds to the warped product of the local approximate form $[AdS_{d+2}]_r \times [\mathbf{K}_k]_r$. Interestingly, most AdS/CFT backgrounds whose geometry is determined by a generic deformation of an UV fixed point admit a representation of the form 2.12, since a single dominant rele-

vant operator will determine a geometry with a single overall curvature scale, both in compact and non-compact factors.

Repeating the calculation of the free fall time for 2.12 we find

$$\tau_* = z_* - z_\beta \sim \beta \, \log \left(b_0 / \bar{\ell}_{\rm P} \right) \ , \tag{2.13}$$

where $\bar{\ell}_{\rm P}$ denotes the Planck length in $d+k+2$ dimensions. On the other hand, the entropy in a single thermal cell reads

$$S_{cell} = \frac{S}{n_{cell}} \sim \frac{1}{VT^d} \frac{1}{\bar{\ell}_{\rm P}^{d+k}} \left(\frac{r_0}{b_0} \right)^d V \cdot V_k(r_0) \ . \tag{2.14}$$

Using $V_k(r_0) \sim b_0^k$ and $T \sim r_0/b_0^2$ we find

$$S_{cell} \sim \left(b_0 / \bar{\ell}_{\rm P} \right)^{d+k} \ , \tag{2.15}$$

so that the main result

$$\tau_* \sim \beta \, \log \left(S_{cell} \right) , \tag{2.16}$$

is obtained in full generality, up to $\mathcal{O}(1)$ coefficients.

Our crucial observation here is that 2.16 is obtained independently of whether we use the $(d+k+2)$-picture or the $(d+2)$-dimensional picture with effective Planck length $\ell_{\rm P}$, obtained by Kaluza–Klein reduction of the compact factor at the horizon $\mathbf{K}_k(r_0)$. The two definitions of Planck length satisfy $\ell_{\rm P}^d = (\bar{\ell}_{\rm P})^{d+k}/b_0^k$, which in turn implies

$$\left(b_0 / \bar{\ell}_{\rm P} \right)^{d+k} = \left(b_0 / \ell_{\rm P} \right)^d \ , \tag{2.17}$$

thus ensuring 2.16 also in the $(d+2)$-dimensional Einstein frame.

2.3 Small systems and topological jumps

A most interesting fact about the past result is the generalization of 2.16 to the degenerate case of $d = 0$, i.e. the situation where the dual system is purely quantum mechanical and the horizon is only extended in 'internal' compact dimensions, so that the previous notion of 'thermal cell' is not defined. In this case one has no alternative to using the $(d+k+2)$-dimensional description, whose the free fall time scales then with the logarithm of the *total* entropy $S \sim (b_0/\bar{\ell}_{\rm P})^k$:

$$\tau_* \sim \beta \log(S) \,. \tag{2.18}$$

A characteristic example of this behaviour is the four-dimensional Reissner–Nordstrom black hole, with near-horizon geometry $\mathrm{AdS}_{1+1} \times \mathbf{S}^2$. In this case the optical depth scales with the logarithm of the full entropy, despite the fact that the size b_0 of the $\mathbf{S}^2$ is much smaller than the inverse temperature β in the extremal $T \to \infty$ limit. Notice that this result for the free fall time must be distinguished from that of the Schwarzschild black hole, despite involving the same formula. The reason is that Schwarzschild black holes have a size of the same order as the thermal length, for any temperature, so that both 2.18 and 2.16 apply to them.

This example suggests that the law 2.16 should be replaced by 2.18 when the system is smaller than the inverse temperature scale. It is interesting to consider examples in which the reduction to a single thermal cell can be achieved by varying a continuous control parameter. The simplest possibility is that of a CFT on a sphere $\mathbf{S}^d$ of radius R. The bulk representation in the high-temperature phase is a large AdS black hole. For $T \sim 1/R$ the black hole has size of $\mathcal{O}(1)$ in units of the AdS curvature and we have a CFT living on a single thermal cell. For $T \ll 1/R$, which corresponds to a system 'smaller' than a single thermal cell, the dominant background is the vacuum AdS manifold, with no horizons. The propagation of bulk signals inside global AdS occurs on the time scale of the order of the curvature radius, i.e. we have a purely 'ballistic' regime for signal propagation on the CFT sphere (recall that the interactions with bulk rad iation are down by one power of $1/N^2$.) This is all natural since the finite size of the sphere gaps the spectrum of the CFT and we only see the vacuum on scales smaller than the thermal length. We conclude that the Hawking–Page transition makes the transition between 2.16 and 2.18 somewhat degenerate in this case, since all low-T entropies are of $\mathcal{O}(1)$ in the large-N expansion.

A more interesting situation would apply if the theory conserves $\mathcal{O}(N_{eff})$ worth of degrees of freedom when system is smaller than a thermal cell. In this case, we need to realize an entropy of $\mathcal{O}(N_{eff}) \sim \mathcal{O}(N^2)$ in a purely quantum mechanical system, i.e. as a black-hole metric of the form 2.12, with $d = 0$. This physical constraint, combined with the Hawking–Page transition in the gapped case, suggests

that we consider large-N phase transitions with the bulk interpretation of topological jumps between metrics of the form 2.12 with a different partition of 'internal' and 'spacetime' directions.

To be more specific, consider the induced geometry at fixed radial variable r and fixed time t, with topology $\mathbf{V}_d \times \mathbf{K}_k$, where $\mathbf{V}_d$ denotes the spatial section of the QFT metric. A topological flop into a system with $d = 0$ has the schematic form $\mathbf{V}_d \times \mathbf{K}_k \to \mathbf{K}_{d+k}$, and will be likely to occur when the three manifolds have about the same proper size at the radius scale set by the horizon $r \sim r_0$, corresponding to a temperature $T \sim r_0/b_0^2$. The size of $\mathbf{K}_k(r_0)$ is given by b_0, whereas the size of $\mathbf{V}_d(r_0)$ is or order $L \cdot r_0/b_0 \sim (LT)b_0$, with L the size of $\mathbf{V}_d$ in the QFT metric. Using the UV/IR relation, these sizes are about equal for $LT \sim 1$, i.e. when the system contains a single thermal cell.

We then expect the quantum-mechanical phase to dominate in the low-temperature regime, $LT \ll 1$, when the system is smaller than a single thermal cell. This is natural since the entropy and/or free energy of the QFT is computed in the bulk prescription by evaluating volume integrals as a function of LT for the two manifolds. At the transition one has $S \sim S_{cell}$, with 2.16 holding at $LT \gg 1$ and 2.18 taking over for $LT \ll 1$. In the next section we consider an specific example of this construction, which in turns provides the effective theory of a single thermal cell.

2.4 The Effective Theory of a Thermal Cell

A particular example of the topological flops described in the previous section can be studied in great detail by using the very explicit solutions of D-brane backgrounds in type II string theories. According to basic AdS/CFT lore, strongly coupled SYM theories in $d+1$ dimensions admit a bulk gravity dual description based on the near-horizon (string frame) metric/dilaton of Dd-branes [24],

$$\begin{aligned} ds^2_{\mathrm{D}d} &= \frac{1}{\sqrt{H_d}}\left(-h(r)dt^2 + d\ell_d^2\right) + \sqrt{H_d}\left(\frac{dr^2}{h(r)} + r^2 d\Omega^2_{8-d}\right) , \\ e^{-2(\phi-\phi_\infty)} &= (H_d)^{\frac{d-3}{2}} , \end{aligned} \tag{2.19}$$

where $H_d = (R_d/r)^{7-d}$ and $h(r) = 1 - (r_0/r)^{7-d}$. This background is a particular case of 2.1, up to a change of coordinates, a Kaluza–Klein reduction on the compact $\mathbf{S}^{8-d}$ sphere, and a final rescaling to an Einstein frame metric.[1] For $\ell_d \in \mathbf{T}^d$, a torus of size L, the associated winding modes become light as $r \to 0$. Resolving this singularity via a T-duality on the $\mathbf{T}^d$ one finds a metric which becomes unstable to localization (a global version of [32, 33]) for $r \ll \alpha'/L$ (see for example [30] for a detailed account). The localized metric is then that of D0-branes, i.e. 2.19 with $d = 0$.

The T-duality transition occurs at the point where local winding modes become of stringy mass, equivalently the local proper size of the spatial torus in the string-frame metric 2.19 is of order

$$L(r_{\alpha'}) \sim L \left(\frac{R_d}{r_{\alpha'}}\right)^{\frac{7-d}{4}} \sim \sqrt{\alpha'} \,. \tag{2.20}$$

The T-dual geometry for $r < r_{\alpha'}$ contains a torus growing towards small r, supporting a uniform distribution of D0-branes. This geometry is globally unstable through the topological 'flop' $\mathbf{T}^d \times \mathbf{S}^{8-d} \to \mathbf{S}^8$. The local size of the warped $\mathbf{S}^{8-d}$ is proportional to r, while that of the T-dual torus is proportional to $\tilde{L} = \alpha'/L$. This determines the location of the flop at $r_{flop} \sim \tilde{L}$, where both fibers have roughly the same size, so that they can have the same action as a round $\mathbf{S}^8$. Since N_{eff} is proportional to the entropy, which in turn scales with the volume of the fibers, our construction guarantees that 2.16 continues to apply in order of magnitude across this transition, where S_{cell} is interpreted in the low-temperature regime as the entropy of the large-N quantum mechanics of the D0-brane system.[2] So we have a system where we go from a law of type 2.16 to a law of type 2.18, with the difference that the low-temperature entropy still shows non-trivial T-dependence.

It is instructive to express these results in terms of SYM variables. Let $\lambda_d = g_{YM}^2 N$ be the 't Hooft coupling of the SYM theory in $d+1$ dimensions. It has length dimension $d-3$ and a dimensionless coupling characterizing the intrinsic strength of interactions at the energy scale T is the running coupling $\lambda_d(T) = \lambda_d T^{d-3}$.

[1] Notice that the D-brane background is of the form 2.12, both in string frame and in Einstein frame.

[2] The entropy computed through the Bekenstein–Hawking formula is invariant under T-duality and also under S-duality.

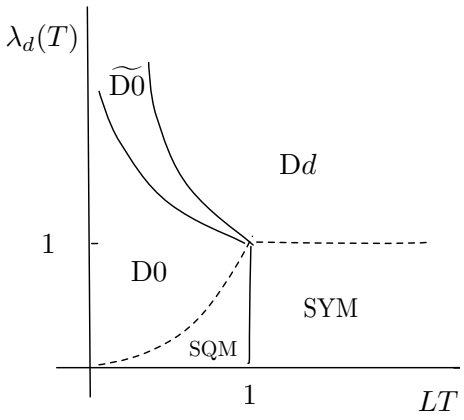

Figure 2.1: Phases of the Dd-brane system as a function of LT and the effective dimensionless coupling in $d+1$ dimensions. In the gravity regimes above the dotted line, we go from the Dd-brane geometry to the smeared D0-brane geometry, $\widetilde{\text{D0}}$, as the torus size goes through the T-duality transition. For even smaller sizes we have a localization transition to the metric of localized D0-branes. The large-N thermodynamic functions are T-duality invariant, and undergo a first-first order phase transition without $\mathcal{O}(N^2)$ latent heat at the localization curve.

The SYM theory can be described by the holographic model 2.19 provided it is sufficiently strongly coupled, i.e. for $\lambda_d(T) \gg 1$, and the temperature is large enough. At temperatures below the critical line $\lambda_d(T) \sim (LT)^{2(d-5)}$, corresponding to $r_0 \sim r_{\alpha'}$, the metric 2.19 must be substituted by the T-dual background of N smeared D0-branes. Further down in temperature the horizon reaches the critical stability line $r_0 \sim r_{flop}$, corresponding to $\lambda_d(T) \sim (LT)^{d-5}$ in YM variables, where the system localizes to the large-N quantum mechanics of N coincident D0-branes, see Figure 2.1. In order to better represent this behaviour, it is useful to define an effective renormalized thermal length ℓ_T, by the relation

$$\ell_T^{5-d} = \frac{\beta^{5-d}}{\lambda_d(T)} \,, \tag{2.21}$$

where strong coupling effects $\lambda_d(T) \gg 1$ make it smaller than the perturbative notion of thermal length of $\mathcal{O}(\beta)$. The expression

$$\tau_* \sim \beta \log(N_{eff}) \,, \tag{2.22}$$

is then valid at all temperatures satisfying the strong coupling condition $\lambda_d(T) \gg 1$, where the effective number of degrees of freedom runs as that of strongly-coupled $(d+1)$-dimensional SYM, see Figure 2.2:

$$N_{eff}(T) = N^2 \left(\lambda_d(T)\right)^{\frac{d-3}{5-d}} \sim \left(S_{|\mathrm{D}d}\right)_{cell} , \tag{2.23}$$

when the size of the system is larger than the effective thermal length $L \gg \ell_T$. For tori smaller than the effective thermal length, $L \ll \ell_T$, we cross-over to the effective number of degrees of freedom of the large-N quantum mechanics at strong coupling:

$$N_{eff}(T) = N^2 \left(\lambda_0(T)\right)^{-\frac{3}{5}} \sim S_{|\mathrm{D0}} , \tag{2.24}$$

with $\lambda_0(T) = \lambda_0 T^{-3}$ the effective dimensionless coupling of the D0-brane system. Using the Kaluza–Klein reduction formula for the SYM theory on the torus, we can write $\lambda_0 = \lambda_d / L^d$, which allows us to express the effective D0 coupling in terms of the original effective Yang–Mills coupling in $d+1$ dimensions through the relation $\lambda_0(T) = \lambda_d(T)(LT)^{-d}$. Notice that the two expressions for N_{eff} match in order of magnitude across the critical transition line $L \sim \ell_T$.

This furnish a specific example interpolating between 2.16 and 2.18 in a smooth way, preserving nicely the expected features of the free fall time scale.

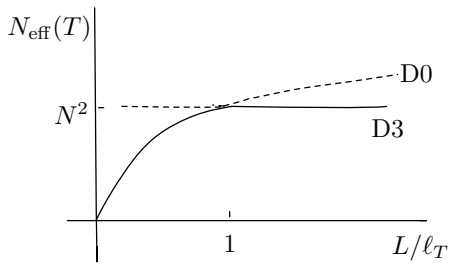

Figure 2.2: Plot of the temperature-dependent value of N_{eff} (full line) as a function of the system size for the SYM_{3+1} theory on a torus. The transition from $N_{eff} = S_{cell}$ to $N_{eff} = S$ occurs at the localization curve, defined by $L \sim \ell_T$. Notice that the dominant solution *m*inimizes N_{eff}, even if it maximizes the total entropy.

2.5 D-branes infalling times

As was commented in the introduction to this chapter, one could argue that the infalling time has been computed for massless excitations, and that other probes, such as D-branes, may show a different result. Indeed this is not the case, and here show that these insightful objects follow the same pattern.

Let us consider a CFT-space filling brane falling rigidly in the bulk metric. The action depends on an effective tension σ and a charge q through

$$I_{brane} = I_{\rm NG} + I_{\rm WZ} = -\sigma {\rm Vol}\,[\Sigma] + q\int_\Sigma A_{\rm WZ}\ , \tag{2.25}$$

where Σ is the word-volume of the brane and $A_{\rm WZ}$ is a Wess–Zumino field coupled minimally to the brane and assumed to be smooth at the horizon. Transforming to Regge–Wheeler coordinates and approximating the action in the Rindler region one finds

$$I_{brane} \approx -\int dt\left(m_{eff}(z)\sqrt{1-\dot z^2}+v_0\right)\ , \tag{2.26}$$

where v_0 is a constant and

$$m_{eff}(z) \approx m_0\, e^{-2\pi T(z-z_\beta)}\ , \tag{2.27}$$

for some positive constant m_0. We see that the effective mass of the brane vanishes exponentially as we approach the horizon. Hence, the fall time from $z = z_\beta$ to the stretched horizon is again of order $z_* - z_\beta = \tau_*$.

Chapter 3

Searching for Fast Scramblers

The purpose of this chapter is to find simple physical models showing Fast Scrambling behaviour. For these matters, we use a pragmatic diffusion approach towards this time scale. Below, we justify this approach under the name of *Probe approximation*. In this framework, we find a *Fast Scrambler* family of models. These physical models are defined on Hyperbolic spaces, and also in their discrete counterparts, so-called expander graphs.

These models will not only be examples of Fast Scramblers, but will have a surprisingly close connection, in a mathematical sense, with black hole physics. We will show this in the following chapter.

The first section develops the concept of scrambling by providing its context and definition. We heuristically connect the fundamental definition with the diffusion approach, which will be one of the tools in the subsequent section. In the last part, we describe another fundamental characterization, in terms of *causality bounds* or *signalling*, connecting with Ref. [34]. In the second section, we apply the diffusion approach to search for fast scramblers. Due to the positive results concerning hyperbolic spaces, we discuss other fundamental approaches to the scrambling time in these spaces, with several interesting insights.

3.1 Generalities

In the context of black hole physics, the notion of *s*crambling is

implicitly associated to the pragmatic situation in which one 'throws in' a small system which qualifies as a perturbation of the black hole state. The combined system is then left to relax in such a way that any information contained in the small initial subsystem is 'mixed' throughout the large set of internal degrees of freedom of the black hole, so that this information becomes only accessible through fine-grained measurements of the final black hole state.

Many subtleties must be faced when trying to formalize the previous paragraph into a concrete mathematical statement. Many of these subtleties result from the tension between the desire to achieve maximal generality and the concrete properties encountered in actual physical systems. This point is quite relevant for our discussion, since black holes cannot be considered to be in the list of 'ordinary' physical systems.

We shall abstain from entering into this intricate conceptual forest, and rather be satisfied with a few brush strokes with the sole purpose of motivating the effective models studied in this work.

Very formally, we can characterize the information content of a quantum system as the degree of knowledge of its quantum preparation, i.e. its degree of 'quantum purity'. A convenient measure of (im)purity is the Von Neumann entropy

$$S_\rho = -\mathrm{T}r\, \rho \log\, \rho\ , \tag{3.1}$$

and the information content can be defined as the negative of this quantity,

$$I_\rho = S_{\mathrm{max}} - S_\rho \tag{3.2}$$

with an additive normalization to a reference maximal entropy for the family of states of interest. For a finite-dimensional Hilbert space $\mathcal{H}$, we can always bound $S_{\mathrm{max}} \leq \log\, \mathrm{d}im\, \mathcal{H}$, although the particular physical set up may suggest other reference normalizations for the 'no information' state, such as for example the microcanonical thermodynamic entropy at fixed energy, or the canonical thermodynamic entropy at fixed temperature.

We say that the state ρ is 'scrambled' when its detailed information content is only accessible to measurements involving essentially all the degrees of freedom of the system. The intuition behind this idea is

that the state is so 'unstructured' that measuring small subsystems gives little clue about the detailed state of the full system.

A subsystem Σ is defined in terms of a tensor factorization of the full Hilbert space, i.e.

$$\mathcal{H} = \mathcal{H}_\Sigma \otimes \mathcal{H}_{\overline{\Sigma}} \tag{3.3}$$

where $\overline{\Sigma}$ is the complementary subsystem. Both Σ and $\overline{\Sigma}$ can be broken up into further subsystems, a process which ends up with the 'elementary degrees of freedom'.[1] A state ρ is said to be scrambled when subsystems smaller than half the total system contain essentially no information about ρ, i.e.

$$I_{\rho_\Sigma} \approx 0 \ , \quad for \quad \mathrm{d}im(\mathcal{H}_\Sigma) < \mathrm{d}im(\mathcal{H}_{\overline{\Sigma}}) \tag{3.4}$$

where ρ_Σ is the state obtained by marginalizing over the complement:

$$\rho_\Sigma = \mathrm{T}r_{\mathcal{H}_{\overline{\Sigma}}}(\rho) \tag{3.5}$$

In [35], Page was able to present an estimate of the right hand side for a system of Q-bits and ρ a globally pure state taken randomly from the full Hilbert space. His result gives

$$I_{\rho_\Sigma} \approx \frac{\mathrm{d}im(\mathcal{H}_\Sigma)}{2\,\mathrm{d}im(\mathcal{H}_{\overline{\Sigma}})} \ , \tag{3.6}$$

again for $\mathrm{d}im(\mathcal{H}_\Sigma) < \mathrm{d}im(\mathcal{H}_{\overline{\Sigma}})$. In practical situations where the degrees of freedom are local in physical space, this quantity is exponentially small in volume factors.

Page's estimate implies that typical states in systems with 'moving parts' contain essentially no information available in small subsystems and serves as a standard: we say that a state is scrambled when it satisfies the Page test with respect to any bi-partition $\Sigma \cup \overline{\Sigma}$, where Σ stands for the smaller factor.

With these simple definitions at hand, we can give a formal characterization of the black hole experiment at the beginning of this section. We start with an Alice system A in a state with high information content, say ρ_A is pure, together with an independent black hole system

[1] When a system is described by a hierarchy of effective theories, the present discussion applies to any one of the effective theories, with a coase-graining procedure relating different levels of description.

in an scrambled state (pure or mixed) $\rho_{\mathrm{B}H}$. The initial combined state is assumed to have no correlations of classical or quantum nature, so that it can be written as

$$\rho_i = \rho_A \otimes \rho_{\mathrm{B}H} \tag{3.7}$$

Hamiltonian evolution of the combined system then results in a final state ρ_f, defined in an slightly enlarged black hole Hilbert space, and having the property of being scrambled in the sense of the Page test. We can represent the result of idealized Page tests on ρ_i and ρ_f by the diagram in Figure 3.1.

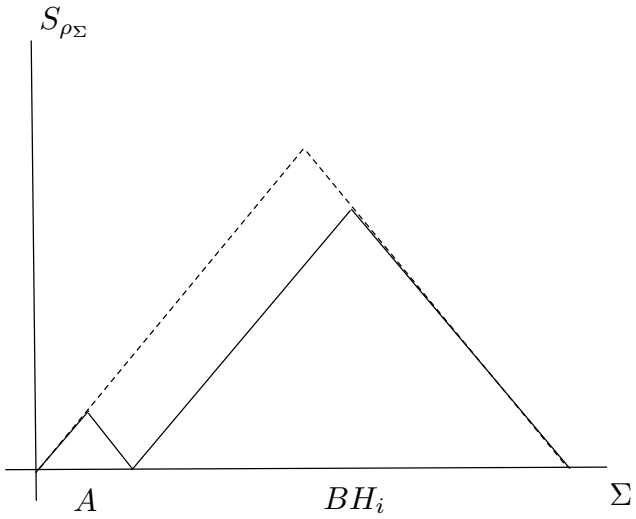

Figure 3.1: The Page test for the initial state $\rho_i = \rho_A \otimes \rho_{\mathrm{B}H_i}$ (full line), versus the Page test for the final state $\rho_f = \rho_{\mathrm{B}H_f}$ (dashed line).

The scrambling time t_S can be defined as the characteristic time scale for the full-line curve in Figure 3.1 to evolve into the dashed-line curve, corresponding to a scrambled state of the combined system after Alice has been absorbed. This definition allows us to interpret the scrambling time as a kind of *g*lobal thermalization time for the full system. It is plain that this time scale depends strongly on the details of the Hamiltonian, such as its degree of locality, as well as the particular choice of subsystem partition. For example, we may expect that information which is locally encoded with respect to a particular factorization scheme:

$$\mathcal{H} = \otimes_j \mathcal{H}_j \tag{3.8}$$

by declaring, say, that Alice corresponds to the first factor $\mathcal{H}_1$, should have different scrambling times depending on the locality properties of the Hamiltonian with respect to this particular basis. Furthermore, the particular choice of observables used to encode and/or measure the information within each $\mathcal{H}_j$ might be relevant when such operators are 'aligned' with structural properties of the Hamiltonian. One such instance appears in [34], where a simple Ising-type qbit system is shown to fast-scramble states that start as completely factorized in local σ_x eigenstates, while doing nothing to states which start as direct products of σ_z eigenstates.

3.1.1 The Probe Approximation

The scrambling time defined above is a very 'involved' quantity, in the sense that the Page test requires gathering a large amount of information about the time evolution of arbitrary subsystems. The general problem of characterizing subsystem evolution is notoriously difficult. While the state ρ of the full system evolves unitarily

$$\rho(t) \longrightarrow e^{-itH}\,\rho(0)\,e^{itH} \tag{3.9}$$

the reduced state $\rho_\Sigma = \mathrm{T}r_{\overline{\Sigma}}\rho$ evolves linearly, conserving the defining properties of a density matrix, i.e. positivity $\rho_\Sigma \geq 0$ and normalization $\mathrm{T}r\rho_\Sigma = 1$. In this case we have a so-called *s*uperoperator, acting as

$$(\rho_\Sigma)_{ab} \longrightarrow \sum_{cd} (\$)_{ab}^{cd}\,(\rho_\Sigma)_{cd} \tag{3.10}$$

where we write indices explicitly to emphasize that \$ acts linearly on the space of density matrices, rather than the Hilbert space of pure states. The \$ operator depends in principle on the full details of the global state on $\Sigma \cup \overline{\Sigma}$, so that the equation (3.10) contains non-local behavior in time from the retarded back-reaction of $\overline{\Sigma}$ on Σ, preventing the existence in general of a local differential equation for ρ_Σ, similar to Schrödinger's. In particular situations when this back-reaction can be neglected or sufficiently averaged by a coarse-graining in the time resolution, the system may have a Markovian description governed by an equation of the type

$$\partial_t \left(\rho_\Sigma\right)_{ab} = \sum_{cd} \mathcal{L}_{ab}^{cd} \left(\rho_\Sigma\right)_{cd} \tag{3.11}$$

where the operator $\mathcal{L}$ is called the Lindbaldian. It describes not only the unitary evolution of ρ_Σ but also the effect of interactions with $\overline{\Sigma}$ through 'quantum jumps'. These terms produce phenomena such as usual energy damping and also decoherence.

From the point of view of (3.11), decoherence is the fast dynamical diagonalization of ρ_Σ by the time evolution. The effective decoherence basis is selected by the interaction Hamiltonian and is responsible for the emergence of classical observables in Σ. Assuming that our time resolution is much larger than the decoherence time for the particular choice of subsystem Σ, we have an equation of Markov type for the diagonal density matrix, which is a probability density over the decoherence basis:

$$\partial_t \, p_i = \sum_j W_i^j \, p_j \tag{3.12}$$

where p_j is now a positive and normalized vector over the particular basis of $\mathcal{H}_\Sigma$ and W_i^j is a matrix of transition probabilities. Positivity and normalization imply $W_i^j \geq 0$ for $i \neq j$ and

$$W_i^i = -\sum_{j \neq i} W_i^j \tag{3.13}$$

for the diagonal entries. Notice that equation (3.12) is similar in structure to Lindblad's (3.11), except that it is written in a smaller configuration space (probability distributions versus full quantum density matrices).

The descent from (3.10) down to (3.12) is rather intricate for any semi-realistic physical system. Examples of systematic analysis in models can be found in the classic works [36–40]. Roughly, one finds that systems with quasiparticles that behave in a semiclassical manner tend to admit a Markovian description of the type (3.12), at least in some limits. Scrambling of any information coded in the quasiparticle position can be characterized by a generalized diffusion problem for the spatial quasiparticle density. This makes contact with the classical description of mixing in an idealized model where particles are described as exercising random walks (brownian motion).

The random walk model of scrambling sacrifices the generality of the Page test and focuses on a specific type of subsystem Σ (akin to a quasiparticle) and a specific basis of states to code the information (i.e. the decoherence basis). Furthermore, if the subsystem Σ is really interpreted as a quasiparticle, it is natural to represent $\overline{\Sigma}$ as having local degrees of freedom accounting for *e*ach elementary transition of the quasiparticle. In this case, we interpret $\overline{\Sigma}$ as a 'quantum lattice' serving as a background for the dynamics of the quasiparticle, with a number of degrees of freedom of the order of the dimension of state-space of the quasiparticle, i.e. a Hilbert space of dimension

$$\mathrm{d}im\left(\mathcal{H}_{\overline{\Sigma}}\right) \sim \exp\left(C\mathrm{d}im(\mathcal{H}_{\Sigma})\right) \tag{3.14}$$

with C some $\mathcal{O}(1)$ constant.

The quasiparticle diffusion model is the benchmark for scrambling at the heuristic level. Since random walks cover a region of size $t^{1/2}$ in a time t, the 'scrambling time' for a uniform system of size L scales as $t_{\mathrm{d}iff} \sim L^2$, with dimensions provided by some combination of microphysical parameters and the effective temperature of the system. If the system is furthermore extensive, we find the standard estimate

$$t_{\mathrm{d}iff} \sim \beta\, S^{2/d} \tag{3.15}$$

with β the effective temperature, up to $\mathcal{O}(1)$ parameters, and S the entropy. The law (3.15) characterizes the scrambling properties of ordinary systems with local quasiparticle excitations.

Needless to say, our command of near-horizon local dynamics in quantum black holes is very far from deriving a simplified model falling under such a restrictive framework. It is nevertheless tempting to propose that information coded in very heavy localized probes, such as infalling D-branes, may admit such a description at a qualitative level. Given the usual terminology of D-branes as very localized *p*robes of space-time, we shall refer to this reduction of the scrambling problem to a generic diffusion problem as the *p*robe approximation. While the detailed justification from some *a*b initio description of the quantum black hole, such as a matrix model or dual gauge theory, is an entirely open problem, we will find it useful to pursue the probe approximation to its limits, adding additional geometrical structure coming from our knowledge of the space-time interpretation of the black hole. One of

the main results of this thesis will be the reconciliation of the simple diffusion model and the exotic (for a diffusion process) dependence on the entropy that is characteristic of fast scramblers.

3.1.2 Scrambling And Signalling

A complementary approach to the study of fast scramblers focuses on the question of 'how fast can they be'. Namely, any fast scrambler must satisfy causality constraints and, indeed, our introduction to fast scramblers in the black hole context emphasizes precisely the 'ballistic' nature of the scrambling. By ballistic we mean here a behaviour with the same scaling as the causally saturating one, being only suppressed by numerical parameters.

Ordinary scramblers conforming to (3.15) do satisfy the causality constraints without problems, since the causal time for local systems scales linearly with system's size, $t_{causal} \sim L$, so that we always have

$$t_{causal} < t_{\mathrm{d}iff} \tag{3.16}$$

for any system larger than one thermal cell, $L > \beta$. This is all that is needed, since the diffusion model itself cannot be defined as such on scales smaller than a thermal cell.

In systems with manifest locality, such as standard QFT, the degrees of freedom are laid down according to a causal geometry with sharp light cones. In lattice approximations to such QFT, the light cones are blurred by short-distance effects, but are still recognizable to $\mathcal{O}(1)$ precision tests. For non-local systems, no simple estimates exist of causal times, and the actual scales may depend very sensitively on details of the Hamiltonian. A principled approach to this problem focuses on the actual physical meaning of causal independence, namely the commutativity of delayed quantum observables. Under a given partition of 'degrees of freedom'

$$\mathcal{H} = \otimes_j \mathcal{H}_j \tag{3.17}$$

we say that observables defined by degrees of freedom 'on i' and 'on j' are *causally connected* after time t if

$$\big[\, O_i(0), O'_j(t) \,\big] = \mathcal{O}(1) \tag{3.18}$$

where the operators are defined in the Heisenberg picture. Physically, this is the condition for a measurement at 'site i' to significantly affect a subsequent measurement done at 'site j' after a time t. The scrambling time is thus bounded-below by the minimal time which achieves (3.18) across all d.o.f. factors.

Very interesting bounds (so-called Lie–Robinson bounds [41]) were proven in [34] for general systems with interactions of matrix-model type (albeit based on bounded operators). In particular, it was shown that the fastest possible signalling time scales *logarithmically* with the number of Hilbert factors in (3.17), in line with expectations for fast scramblers. Notice that no locality of the Hamiltonian is assumed in establishing these bounds.

We shall see that signalling bounds also play an interesting role in those systems that are able to fast-scramble probes, along the lines of the previous section. In particular, one of the main results of this thesis will be the observation that the scrambling time may satisfy *upper bounds* under some idealized situations.

3.2 Diffusion, Random Walks and Graphs

We begin by developing the *phenomenology* of Random Walks in graphs and diffusion in continuous manifolds. The space-time background or the *adjacency matrix* of a graph codify the structure of interactions of the Hamiltonian.

We first review the subject of random walks on graphs, focusing on necessary items and referring to other places for deeper analysis. Then we show the closed connection of this problem with diffusion in continuous manifolds.

In the second part, we explore *Euclidean* cases. We follow by developing the more compelling *expanding* ones.

3.2.1 Generics of Walks

The problem of a random walk in an abstract graph is a famous and recurring problem in both mathematics and physics. It is concerned with the dynamics of a certain object which can be located in N different positions. The description of that object at a given instant of time is given by means of a probability distribution, providing the

probabilities of finding the object in each of the N locations. Therefore, the object is described by a vector p_i of N components, which must satisfy the probability constraint, given by $\sum_{i=1}^{i=N} p_i = 1$.

The dynamics is defined by means of a Markov process. This is carried out by a linear transformation, which is usually called the transition matrix. We have a simple law of the following form:

$$p_j^{n+1} = Mp^n = \sum_{i=1}^{i=N} M_{ji} p_i^n \ , \tag{3.19}$$

where $\sum_{j=1}^{j=N} M_{ji} = 1$, so that evolution conserves the probability constraint, and $M_{ji} = M_{ij}$ due to microscopic reversibility. This condition is a special case of the general *detailed balance*, which occurs when the degeneracy of each possible state equals one. The physical picture is that of a particle moving on a graph[2], from vertex to vertex, with probabilities given by the entries of the matrix M.

Given that we have a probability distribution, we can assign an entropy to each particular state, quantifying our knowledge of the position of the particle. This is the celebrated Shannonś entropy, given by

$$S_p = -\sum_{i=1}^{i=N} p_i \log(p_i) \ . \tag{3.20}$$

This entropy is equal to zero when the object is sharply localized at a certain position and is maximal in the uniform distribution given by

$$u_i = 1/N \ , \tag{3.21}$$

where the entropy equals $\log(N)$. From this perspective, this entropy should be interpreted as a thermodynamical entropy. In a parallel setting, within the quantum mechanical framework of the past section, one is able to interpret it as the entanglement entropy of the

[2]A graph is collection of *vertices* and a collection of *edges* between them. The graph can also be *weighted*, in the sense that we can give different *weights* to different edges

algebra of operators of size $\log(N)$ defining the *probe* observable. One can show that the Markov process injects entropy at each time step, carrying whatever initial probability distribution to the uniform distribution. In other words, the process tends to maximize this entropy function and, therefore, the entanglement entropy of this abstract partition of the quantum state.

This uniform distribution is also called the stationary distribution. This is because it is the only physical eigenstate of the transition matrix, and it has eigenvalue 1. Consequently, it does not evolve with time and all other physical states evolve towards it.

Knowing the spectral decomposition of the transition matrix amounts to solve

$$Mv_a = \lambda_a v_a \ , \tag{3.22}$$

where we will set $\lambda_u = 1$ corresponding to $u_i = 1/N$.

Due to detailed balance, we know that this should provide us with a basis of eigenvectors, expanding the space of probability distributions. At the same time, one can easily check that the coefficient in front of the uniform distribution is fixed to 1 for any physical probability distribution (the sum of probabilities must add to one). Therefore

$$p^0 = u + \sum_{i=1}^{i=N-1} c_a v_a \ , \tag{3.23}$$

where p^0 is a generic initial probability distribution. Plugging this into the evolution equation, after n time steps we have

$$p^n = u + \sum_{i=1}^{i=N-1} c_a (\lambda_a)^n v_a \ . \tag{3.24}$$

The row stochastic nature of the transition matrix implies (Perron-Frobenius theorem) that the absolute value of any of the other eigenvalues is less than one, an essential ingredient for the attainment of equilibrium, for obvious reasons. With this in mind, we consider, without loss of generality, that $1 \geq |\lambda_1| \geq |\lambda_2| ... \geq |\lambda_{N-1}|$. From here we can already bound the difference with respect to the uniform distribution by

$$|p^n - u| = |M^n(p^0 - u)| \leq |\lambda_1|^n |p^0 - u)| \leq |\lambda_1|^n = (1 - \Delta)^n \ , \quad (3.25)$$

so that the figure of merit in this problem is the gap of the transition matrix Δ. This gap controls the rate of approach to equilibrium of the probability distributions.

In order to show the connections with the continuum case, we need to be more specific with the form of the transition matrix. In particular, we fix the degree of connectivity of each vertex [1] to k. This imposes a discrete analogue of homogeneity in the underlying graph. We also impose the analogue of isotropy, which amounts to say that transition probabilities out of a given vertex are equal to one another. Denoting by $r \in [0, 1]$ the probability of *no jump* we have

$$M = \frac{1 - r}{k} A + r \ , \quad (3.26)$$

where A is the adjacency matrix of the graph [2]. In the case at hand, we have a simple k-regular graph of N vertices. It can be proved that such adjacency matrices have a spectrum contained in the interval $[-k, k]$ [42]. The lower bound can only be achieved for bipartite graphs, which will not be considered for simplicity here.

Now we can define the analogues of the continuous gradients and divergences for the discrete graph [42]. In particular, one can define the analogue of the Laplacian in continuous manifolds, called the graph Laplacian, which reads:

$$\Delta \equiv 1 - \frac{1}{k} A \ . \quad (3.27)$$

This a positive-definite matrix with eigenvalues in the interval $[0, 2]$. The uniform distribution is the zero mode of this Laplacian, and the second largest eigenvalue directly defines the gap.

Rewriting the past Markov chain relation in terms of this new matrix

$$p^{n+1} - p^n = -(1 - r)\Delta p^n \ , \quad (3.28)$$

[1] *Fix* is to be understood in relation to the thermodynamic limit

[2] $A_{ij} = 0$ if i, j are not connected by an edge and $A_{ij} = 1$ if they are

we arrive to the discrete analogue of the usual diffusion equation in continuous manifolds.

$$\partial_t p = D\nabla^2 p \, . \tag{3.29}$$

Although it is not so common to treat the continuum case as we have treated the discrete case, it can indeed be thought in the same way, arriving to the conclusion that the Laplacian gap of the model controls the rate of attainment of equilibrium.

3.2.2 Euclidean nets

To begin with, we describe an easy example: a random walk in a flat lattice. This is the discrete analogue of diffusion in flat space-time. The mother of the diffusion laws is the known dispersion relation $L \sim \sqrt{t}$ for the spreading of the probability distribution. For extensive systems we have $S \sim L^d$, so that we expect scrambling times of $\mathcal{O}(S^{d/2})$.

To review how to recover this result from the technology of the past section, we need to compute the gap of a d-dimensional net. Supposing that the net has periodic boundary conditions, the biggest wavelength is $\lambda_{max} = L$ so that $\Delta = \frac{4\pi^2}{L^2}$. For the so-called lazy random walk [3], $r = 1/2$, we have then

$$|p^n - u| = (1 - \frac{1}{2}\Delta)^n \, , \tag{3.30}$$

which goes to zero for $t_{flat} \gg N^{2/d} \sim S^{2/d}$.

We can repeat the argument for the continuum case. For simplicity and future reference, we study the diffusion equation in the half line, so that we need to solve

$$\partial_t p = D\frac{\partial^2}{\partial x^2} p, \tag{3.31}$$

where $x, t \in [0, \infty)$ and the initial condition is that of sharply localized perturbation at $x = 0$, so that $p(x, 0) = \delta(x)$.

The solution is given by the following Gaussian distribution

[3] We specify to this value to avoid certain technicalities concerning convergence to the stationary distribution, but this choice does not affect any of the results

$$p = \frac{1}{\sqrt{4\pi D t}} e^{-\frac{x^2}{4Dt}} \ , \tag{3.32}$$

which is centred at $x = 0$ for every moment of time, and which has a width $\sigma = \sqrt{2Dt}$, providing the origin of the relation $L \sim \sqrt{t}$, and therefore signalling the slow scrambling nature of these spaces.

3.2.3 Expander graphs and hyperbolic spaces

We have seen that the origin of the polynomial law, typical of a slow scrambler, is the polynomial vanishing of the spectral gap in these flat spaces. So if we want to decrease the diffusion time we need to increase the spectral gap of the theory in the thermodynamic limit. Luckily, there is an insightful family of graphs whose gap remains fixed as we take this infinite size limit. These are the so-called expander graphs and feature prominently in graph theory, due to their numerous applications to several branches of mathematics [42, 43].

Indeed one of the central results in expander graph theory is the fast mixing of random walks. Using the past framework and the fact that the gap is bounded away from zero in the thermodynamic limit, which we name by Δ_∞, we can bound the distance (3.30) by $1/N^\alpha$ with $\alpha > 0$, just by setting $n > C \log(N)$, where C is a positive numerical constant proportional to $-\alpha/\log(1 - \Delta_\infty/2)$.

In the mathematical argon these are two out of three possible and equivalent definitions of a expander graph, regarding the focus on the algebraic or probabilistic nature of these intriguing objects. The third possibility regards the combinatorial properties of them. We can bring it here with the aid of a known geometrical interpretation of the Laplacian gap, as a consequence of the so-called Cheeger inequality

$$\frac{h^2}{2} \leq \Delta \leq 2h \ , \tag{3.33}$$

where the Cheeger constant, h, is the (normalized) edge expansion of the graph, defined as the formal ratio of 'area/volume',

$$h \equiv min \ \frac{\#\, edges\, [\, \partial\, S\,]}{k\, N_S} \ , \tag{3.34}$$

and where the minimum is taken over all graph bi-partitions $G = S \cup (G - S)$, with the proper subgraph S having vertex size N_S smaller

than half of G, i.e. $N_S \leq N/2$. In the numerator it is counted the total number of edges connecting the two sides of the partition, thus measuring the boundary volume in edge units. Therefore, an expander graph family has a bounded finite h in the large N limit, implying that large subsets have a boundary volume scaling as their bulk volume. We then naturally recognize expanders as the discrete analogue of hyperbolic geometry.

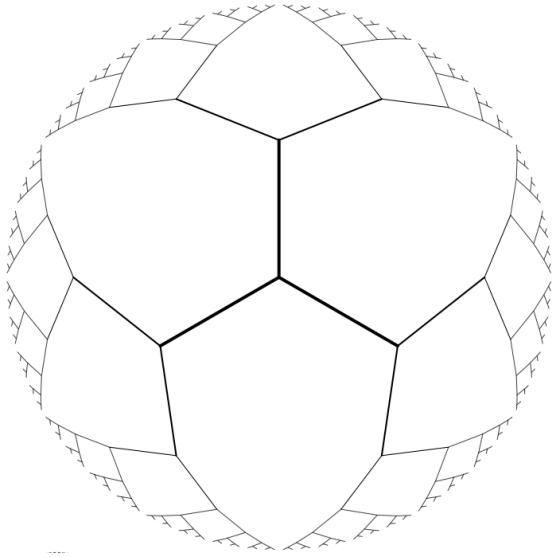

Figure 3.2: The infinite regular tree, or Bethe lattice, is the ultimate expander. Its adjacency matrix has a continuous spectrum in the interval $[-2\sqrt{k-1}, 2\sqrt{k-1}]$. The figure shows the case $k = 3$, a tessellation of the two-dimensional hyperboloid.

For example, the simplest and in many ways the most perfect expander is a regular tessellation of the Hyperbolic space $\mathcal{H}^{k-1}$, known as the Cayley tree or Bethe lattice (cf. Figure 3.2). The metrical properties of the k-regular Bethe lattice give an approximation of the $(k-1)$-dimensional unit hyperboloid

$$ds^2_{\mathcal{H}^{k-1}} = dr^2 + (\sinh\, r)^2\, d\Omega^2_{k-2}\ , \tag{3.35}$$

with lattice spacing of order unity.[4] We can introduce hyperbolic

[4]Continuum models of finite expander graphs can be constructed as compact

spaces of arbitrary curvature radius R, just scaling this metric by a factor of R^2, and the corresponding Bethe lattice would have spacing of $\mathcal{O}(R)$.

This analogy suggest that the continuum analogue of this problem should also show certain fast scrambling insights. The diffusion equation in curved space is just

$$\partial_t p = D\frac{1}{\sqrt{g}}\partial_\mu(\sqrt{g}g^{\mu\nu}\partial_\nu)p \ . \tag{3.36}$$

We will consider spherically symmetric configurations, so that $p = p(r,t)$. In this case the diffusion equation in hyperbolic space or radius R takes the following form

$$\partial_t p = D\frac{1}{senh(\frac{z}{R})^{k-2}}\partial_z((senh(\frac{z}{R})^{k-2}\partial_z)p \ , \tag{3.37}$$

where we have rescaled the radial variable $z = rR$. The exact solutions to this equation can be found in [44]. We quote here the solution in three spatial dimensions (which is equivalent to setting $k = 4$), which happens to take a particular simple form

$$p_3(z,t) = \frac{e^{-\frac{Dt}{a^2}}}{8R(\pi Dt)^{\frac{3}{2}}}\frac{ze^{-\frac{z^2}{4Dt}}}{senh(z/a)} \ . \tag{3.38}$$

In contrast with the flat diffusion solution, this is a Gaussian distribution whose peak moves radially with a velocity $v_{\text{peak}} = \frac{2D}{R}$, a fact that can be easily checked by completing the square of the exponents when $z \gg R$. Therefore the perturbation moves ballistically over the manifold.

In fact, focusing our attention in the probability density of being at a certain distance z from the origin at time t, which we call $p_z(z,t)$, we have

$$p_z(z,t) = V_{\mathcal{S}^{k-2}}(R\sinh(z/R))^{k-2}p(z,t) \ . \tag{3.39}$$

This probability distribution satisfies then a Fokker-Planck type equation

---

hyperbolic manifolds of the form $\mathcal{H}^{k-1}/\Gamma$, with Γ a free discrete subgroup of isometries.

$$\partial_t p_z(z,t) + \partial_z(v \cdot p_z(z,t)) = D\partial_z^2 p_z(z,t) \ , \tag{3.40}$$

with drift velocity $v = \frac{(k-2)}{\tanh(z/R)}\frac{D}{R}$. This velocity approaches exponentially fast its limiting value $v_\infty = (k-2)D/R$ as $z \gg R$. In the three dimensional case, $k = 2$ and we recover the past result. This, as was pointed out in [44], can be interpreted as a biased Random Walk in the half line, explaining the ballistic nature of the diffusion in the radial direction.

So, generically, for any dimension, perturbations in an hyperbolic space spread ballistically. Now we can join this interesting feature with the fact that volume increases exponentially fast in these spaces. Supposing an extensive system we have $S \sim V \sim e^L$, where L is the size of the system. Therefore we need to travel a distance $\mathcal{O}(\log(S))$, which we do in $\mathcal{O}(\log(S))$ due to the ballistic behaviour. This can be argued as well for the discrete expander case just by appealing to the known fact that the size of an expander graph of N vertices is of order $\mathcal{O}(\log(N))$, equal to the mixing time, so that mixing in these graphs saturate causality bounds.

At the same time, as expected, the analogy between this continuum and discrete structures goes also to the algebraic properties of the Laplacian. It is well known that the wave equation in the non-compact hyperbolic space has a bounded gap, of the order of the radius of curvature for any dimension. This provides another way to show fast diffusion in this continuous manifolds.

In this little section we have argued in several ways that expanding structures, such as expander graphs or hyperbolic spaces, are natural fast scramblers. The key property is that the spectral gap remains bounded away from zero in the thermodynamic limit. This, in turn, through the Chegger inequality, is intimately connected with the expansion of the underlying structure.

3.3 Quantum approaches in Hyperbolic spaces

In the past section we have taken a coarse grained approach to study the scrambling time. In particular we have step on a heuristic defini-

tion of a probe, which should furnish a subspace of dimension equal to the entropy of the full Hilbert space. There are some clear drawbacks to this approach. One is the lack of rigour in the operational definition of this probe and in the derivation of its effective equation, when a coarse graining in time is applied. Another one is the arbitrariness of the partition.

We would like to free ourselves of these drawbacks and develop some approach nearer the quantum mechanical ideas which gave rise to the scrambling time, or at least nearer the quantum mechanical framework in general, without any simplifying approximations. In principle one should expect a rigorous path to define the probe and derive its equation but, lacking this procedure, we will try to approach the scrambling time in two other different ways.

In particular, having in mind the past section results we go on study several properties of quantum models defined on expanding spaces. We obtain some positive results concerning propagation of information in these spaces and some negative ones, although interesting, when trying to apply the page test to expander graphs.

3.3.1 Entanglement entropy in expander graphs

In this first section we study some generic properties of entanglement entropy in quantum models defined on expander graphs. We make no explicit reference to a probe subsystem or any other quasiparticle degree of freedom. Rather, we focus on generic properties of entanglement with respect to bi-partitions of the expander graph, and point out some difficulties concerning the Page test definition of the scrambling time.

Let then G be a connected graph where a local quantum system is defined, and $A \cup \bar{A}$ a bi-partition into two connected components, with the convention that A has the smaller vertex size: $N_v(A) \leq N/2$. Given a general state on G, described by a density matrix ρ, we can define the usual marginal density matrix of A and its entanglement entropy

$$\rho_A = Tr_{\bar{A}}\, \rho \,, \qquad S_A = -Tr_A\, \rho_A \log \rho_A \,. \tag{3.41}$$

As was described in the first section of this chapter, a natural criterion to declare a system as scrambled is to demand that S_A be

bounded below by some fixed extensive function, for all choices of A under the stated conditions,

$$S_A \geq C\, N_v(A)\ , \qquad N_v(A) \leq N/2\ . \tag{3.42}$$

For systems with finite-dimensional Hilbert space at each vertex, this criterion is then equivalent to maximal mixing of ρ_A when the constant C saturates to its upper bound $C_{max} = \log \dim \mathcal{H}_v$. In other cases, it incorporates the fact that we may have different effective temperatures depending on the total energy of the state or that our computational abilities just allow us to find the scaling. This extensive condition for the entanglement entropy of a quantum state was referred as the Page criterion [35], leading to a natural definition for the scrambling time [5], [6], [34], [3]. It is the typical lapse of Hamiltonian evolution needed to satisfy the Page criterion, starting from an initial state which explicitly violates it.

With this in mind we may focus on globally pure states on G. Two possibilities emerges for good candidates of non-scrambled states, *which explicitly violates the Page criterion.* Possibly the best choice for the 'least thermalized' initial state may be a completely factorized one $\otimes_v |\psi_v\rangle_v$, for which $S_A = 0$ for all partitions. Such type of initial states where also considered in [34] with similar type of objectives in mind. The second natural choice of initial state is one whose entanglement properties imitate those of the ground state. For systems with short-range correlations such ground states satisfy the so-called 'area law' for the entanglement entropy, i.e. $S_A \sim size[\,\partial A\,]$, where $size[\,\partial A\,]$ can be measured in terms of the edge size of the boundary, $N_\ell(\,\partial A\,)$, for k-regular graphs. Within these type of states and partitions the usual intuition about quantum thermalization suggests then that the scrambling consists on the gradual evolution from 'area law' to 'volume law' for the entanglement entropy of spatial domains.

Already at the level of these primitive notions, we see that expander graphs are special in their behavior with respect to extensivity. In particular, there is no clear-cut distinction between 'area-law' and 'volume-law' behaviors when G is an expander. As a consequence of the expansion property (3.34), any area-law entanglement entropy of a bi-partition $G = A \cup \bar{A}$ satisfies the Page criterion

$$S_A = s_A\, N_\ell(\,\partial A\,) \geq h\, k\, s_A\, N_v(\,A\,) \tag{3.43}$$

from the beginning. Such 'area-law' states are not difficult to engineer and do not look 'thermal' at all. Moreover, as we will show, they can be prepared in a time scale of $O(\beta)$, which would provide a clear counterexample to the Fast Scrambling conjecture.

To illustrate these facts, let us consider a simple Hamiltonian with localized vertex terms and 'hopping' interactions for each edge of the graph,

$$H = \sum_{v \in \, vertices} h_v + \sum_{\ell \in \, edges} h_\ell \ , \tag{3.44}$$

where h_v acts on the single-vertex Hilbert space $\mathcal{H}_v$ and the hopping term h_ℓ acts on the two-vertex Hilbert space $\mathcal{H}_\ell = \mathcal{H}_\sqsubset \otimes \mathcal{H}_\sqsupset$ associated to the edge $\ell = (vw)$. Let us suppose now that $h_\ell \ll h_v$ and construct the ground state in the hopping expansion in powers of λ, a small parameter characterizing the matrix elements of h_ℓ. To zeroth order, the vacuum is determined by the on-vertex vacua $|0\rangle_v$ for each operator h_v,

$$|Vac\rangle = |\,\Pi\,\rangle + \mathcal{O}(\lambda) \equiv \otimes_v \, |0\rangle_v + \mathcal{O}(\lambda) \ , \tag{3.45}$$

a completely factorized state for which $S_A = 0$ for any bi-partition. To leading order in the hopping terms the ground state has the form

$$|Vac\rangle = \alpha \, |\,\Pi\,\rangle + \lambda \sum_{\ell \, \in \, edges} |\,\ell\,\rangle + \mathcal{O}(\lambda^2) \tag{3.46}$$

where the sum extends over all links $\ell = (vw)$ of the lattice G and the state $|\ell\rangle$ differs from the completely factorized on-site vacuum $|\Pi\rangle$ by an excitation on the ℓ-edge Hilbert space $\mathcal{H}_\ell = \mathcal{H}_v \otimes \mathcal{H}_\sqsupset$. It is orthogonal to the zeroth-order vacuum, $\langle\,\Pi\,|\,\ell\,\rangle = 0$, and its particular form is determined by the matrix elements of h_ℓ through the usual formulae of first-order perturbation theory. Normalization sets the constant α to the value $\alpha = \sqrt{1 - \lambda^2 N_\ell}$, with N_ℓ the total number of edges in G.

Given now a bi-partition $G = A \cup \bar{A}$, we define the state

$$|\lambda_{A^o}\rangle = \sqrt{\alpha} \, |\,\Pi_{A^o}\,\rangle + \frac{\lambda}{\sqrt{\alpha}} \sum_{\ell \in A^o} |\,\ell\,\rangle \ , \tag{3.47}$$

where the link sum includes only those edges lying entirely within the interior A^o of the subgraph A and $|\,\Pi_{A^o}\rangle = \otimes_{v\in A^o}|0\rangle_v$. Using this state we can write the vacuum to leading order in the hopping expansion as

$$|Vac\rangle = |\,\lambda_{A^o}\,\rangle \otimes |\,\lambda_{\bar{A}^o}\,\rangle + \lambda \sum_{\ell_\partial} |\,\ell_\partial\,\rangle + \mathcal{O}(\lambda^2)\ , \tag{3.48}$$

where ℓ_∂ denotes edges on the boundary ∂A.

In other words, the vacuum remains factorized except for $\mathcal{O}(\lambda)$ non-trivial excitations localized on the boundary of the partition. It follows that the entanglement entropy of the partition is proportional to the number of edges on the boundary, i.e.

$$S_A = \lambda\, c\, N_\ell(\partial A) + \mathcal{O}(\lambda^2)\ , \tag{3.49}$$

with c a positive numerical constant.

Hence, we recover the expected result: ground states with very short-range correlations have 'area-law' entanglement across bi-partitions.

The peculiar behaviour of expander graphs regarding Page-like criteria can be further emphasized by looking at the opposite limit, in which we regard the vertex Hamiltonian density as negligible compared to the hopping term, i.e. in the limit $|h_v| \ll |h_\ell|$. Let us assume that the Hamiltonian is homogeneous, in the sense that h_ℓ is given by the same operator for all links, so that $[h_\ell, h_{\ell'}] = 0$ for all links on G. Then, the evolution operator can be approximated as

$$U_G(t) = \prod_{\ell\,\in\, edges} U_\ell\ , \qquad U_\ell = e^{-ith_\ell}\ , \tag{3.50}$$

with h_ℓ independent of ℓ, so that the ordering in the operator product is actually immaterial. If the initial state is still given by the factorized ground state of the h_v Hamiltonian, $\otimes_v|0\rangle_v$, since in general $[h_v, h_\ell] \neq 0$ when $v \in \ell$, we see that each link operator U_{vw} will generate entanglement in the $\mathcal{H}_v \otimes \mathcal{H}_w$ subspace in a time scale set by the eigenvalues of h_ℓ. Since h_ℓ is interpreted as the hopping operator, we call β the characteristic time scale for its inverse normal frequencies. The resulting state with $\mathcal{O}(1)$ entanglement across links is generally termed a *graph state* in the literature (cf. [45]), and its entanglement entropy is of the order of the rank of the off-diagonal

adjacency sub-matrix connecting A and $\bar{A}$. For a regular graph with fixed coordination k, this so-called 'Schmidt rank' is of the order of the boundary edge-size, $N_\ell(\,\partial A\,)$, up to k-dependent degeneracy factors.

We thus conclude that hopping-dominated Hamiltonians on regular graphs achieve the *graph state* with area-law entanglement in times of $\mathcal{O}(\beta)$. If the regular graph is also an expander, then we satisfy the Page criterion in 'scrambling' times of $\mathcal{O}(\beta)$. To sharpen more this construction consider taking $\mathcal{H}_v$ to be a two-level quantum system and h_ℓ determined by a single fundamental frequency of time scale β, the evolution operator (3.50) is actually periodic on time scales of $\mathcal{O}(2\beta)$, so that its putative Poincaré recurrence time scale is extremely small, making it hard to talk physically about 'scrambling' or any type of thermalization for that matter. [5]

The solution to this conundrum seems to be in the subtle prefactor going in front of the extensive scaling of the entanglement entropy. What we are seeing is that there are systems for which this prefactor has to be computed exactly. In particular, another reason confirming that these previously constructed states are not scrambled states, is the following. The initial state is of the form $\otimes_v |0\rangle_v$, which, formally, can be expressed in the form

$$|\psi\rangle = |0\rangle_i \otimes \Pi_{v\neq i} \otimes_v |0\rangle_v = |0\rangle_i \otimes |\psi\rangle_{v\neq i}\ , \tag{3.51}$$

In other words, we can consider that we are codifying the vacuum state in one of the vertices, and we want to study how the evolution *scrambles* this information. Here, *scrambles* means that the evolution codifies that information in a subspace of the Hilbert space whose size is of the order of the full Hilbert space, so that for recovering that Information we need to access $\mathcal{O}(N)$ degrees of freedom of the system. In our case, it is clear that the evolution does not achieve this *codification* in one step. In times of $\mathcal{O}(\beta)$ each node has interacted just with its adjacent nodes. The information concerning the initial vacuum state has been delocalized very mildly, and indeed it should be extracted by just measuring the specific node and its neighbours. This is, in other words, an expression of causality in the theory defined of the expander graph. In this way we see that, although globally the

[5] The same can be said about the random Ising model example presented in [34]. In that case the scrambling time is of $\mathcal{O}(\log N)$ because it takes $\mathcal{O}(\log N)$ time steps to build a random lattice with $\mathcal{O}(\log N)$ average vertex degree.

state seems scrambled, one can locally verify clearly that this is not the case [6].

3.3.2 Causal properties of hyperbolic thermal states

Given the previous comments we see that the *Page* test can be a misleading approach if exact computations of the entanglement entropy are not attainable. On the other hand, we see that propagation of the information seems to be a more reliable phenomenon and, as commented in the first section, it clearly provides lower bounds for the scrambling time.

In this way it might be interesting to look for alternative characterizations of the 'ballistic' nature of expander-diffusion, without making any type of approximation or coarse graining. The diffusion model based on random walks assumes the stability of the walking probe. This in turn is equivalent to the assumption that the system has a conserved quasiparticle density or, more generally, a locally conserved current. On general grounds, retarded correlation functions of such local currents will show a characteristic 'diffusion pole' in the lower half plane of complexified frequencies. For local diffusion on an Euclidean geometry with diffusion constant D, such a pole takes the form $\omega_{diff} = -i\, D\, \vec{k}^{\,2} + \dots$ in a large wavelength expansion. Setting $|\,\vec{k}\,| \sim 1/L$ for a fluctuation of wavelength L, we find the standard diffusion time scale $D^{-1}L^2$ of a slow scrambler.[7]

This behaviour of retarded correlation functions is expected to be quite different when the diffusion takes place in an expander graph. As a preliminary discussion, we may look at the continuum approximation and concentrate on the behaviour of retarded correlation functions for field theories on hyperbolic manifolds. A first indication in this direction is the behaviour of the free-field conformal Green's functions on hyperbolic space-times of the form $\mathbf{R} \times \mathbf{H}^n$, with the first factor representing a time-like dimension.

[6] The same can be said about the system studied in [34] in which initially locally codified information is delocalized into $\mathcal{O}(\log N)$ degrees of freedom in $\mathcal{O}(\log N)$ time, so that recovering it just amount to measure those $\mathcal{O}(\log N) \ll N$ degrees of freedom.

[7] This diffusion quasi normal mode is visible in the gra vitational description of hydrodynamics, even if a quasiparticle picture is absent in this framework, provided D is of $\mathcal{O}(1)$ in the large N limit.

$$G_{ret}(t,x) = \left\langle 0,0 \left| \left(\partial_t^2 - \nabla^2_{\mathbf{H}^n} + \frac{n-1}{4n} R_{\mathbf{H}^n} \right)^{-1} \right| t,x \right\rangle_{ret} \tag{3.52}$$

$$\sim \delta(t - L_x) \, \frac{1}{(\sinh L_x)^{n-2}} \, , \tag{3.53}$$

where $(t,x) \in \mathbf{R} \times \mathbf{H}^n$ and L_x is the hyperbolic geodesic distance from the conventionally chosen origin of coordinates on $\mathbf{H}^n$ to the point x (cf. for example [46]). We see that the retarded correlation function is indeed *ballistic*, since it is strictly supported over the past light-cone of the origin, despite the presence of a constant-curvature term which simulates a mass. Furthermore this Green function is *automatically thermal*, since it is periodic under imaginary-time shifts $t \to t + 2\pi i$ when integrated against arbitrary sources. The effective temperature for a hyperboloid of radius R is then $\beta^{-1} = (2\pi R)^{-1}$.

The fact that perturbations on a free system behave ballistically at finite temperature is not surprising. After all, the retarded Green function of any free field theory is a c-number, being proportional to the commutator function of free fields, and thus it is the same in any state. On the other hand, the functional form in (3.52) is largely dictated by conformal symmetry, and in particular the hyperbolic Green function must be proportional to the vacuum Green function on Minkowski space, since $\mathbf{R} \times \mathbf{H}^n$ can be conformally mapped into a proper region of $\mathbf{R} \times \mathbf{R}^n$, given by the causal development of the unit ball $\mathbf{B}^n$ on the $t = 0$ spatial section $\mathbf{R}^n$. This region of Minkowski space, denoted $\mathcal{D}(\mathbf{B}^n)$, has the form of a 'diamond' based on $\mathbf{B}^n$.

This fact suggests a very interesting and non-trivial generalization of (3.52) to the case of fully interacting (but still conformal) field theories. It is known (cf. for example [47] [48]) that a CFT thermal state of temperature $1/2\pi$ on $\mathbf{R} \times \mathbf{H}^n$ is conformally related to a vacuum state on $\mathbf{R} \times \mathbf{R}^n$ in the following sense: any time-dependent correlation function on the *hot* hyperboloid is conformally related to a *vacuum* Minkowski correlation function, *restricted* to $\mathcal{D}(\mathbf{B}^n)$.

Denoting $\eta_{\mu\nu}$ the Minkowski metric on $\mathbf{R} \times \mathbf{R}^n$ and $g_{\mu\nu}$ the hyperbolic metric on $\mathbf{R} \times \mathbf{H}^n$, we write $\eta_{\mu\nu} = \Omega^2 \, g_{\mu\nu}$ for the conformal rescaling. It turns out that the whole hyperbolic space-time is mapped to the finite domain $\mathcal{D}(\mathbf{B}^n)$ of Minkowski space-time.

More explicitly, if the Minkowski metric is written as

$$\eta_{\mu\nu} = -dt^2 + dr^2 + r^2 d\Omega_{n-1}^2 \tag{3.54}$$

and we perform the following coordinate transformation (which is valid just on $\mathcal{D}(\mathbf{B}^n)$)

$$t = R\frac{\sinh(\tau/R)}{\cosh u + \cosh(\tau/R)} \tag{3.55}$$

$$r = R\frac{\sinh(u)}{\cosh u + \cosh(\tau/R)} \tag{3.56}$$

we arrive to

$$\eta_{\mu\nu} = \Omega^2[-d\tau^2 + R^2(du^2 + \sinh^2(u)d\Omega_{n-1}^2] \tag{3.57}$$

with

$$\Omega = (\cosh u + \cosh(\tau/R))^{-1} \tag{3.58}$$

Now, the Minkowski vacuum, as measured by local correlation functions restricted to $\mathcal{D}(\mathbf{B}^n)$, is equivalent to the mixed state obtained by tracing over the degrees of freedom 'outside' the unit ball, i.e. we may replace the Minkowski vacuum by the entanglement density matrix on the unit ball. We therefore wish to follow the conformal map for this density matrix, to obtain the state in the Hyperbolic version of the theory. As a matter of fact, since every density matrix is hermitian and positive definite, they can be formally expressed as $\rho = e^{-H_M}$ where H_M is the so-called *Modular Hamiltonian*. So, formally, every density matrix is a *thermal* state with $\beta = 1$, with respect to its modular Hamiltonian. Moreover, this modular Hamiltonian is the generator of a symmetry of the system, as can be seen by

$$\mathrm{tr}(\rho U(s)\mathcal{O}U(-s)) = \mathrm{tr}(\rho\mathcal{O}) \tag{3.59}$$

with $U(s) = e^{-iHs}$

This abstract *flow* is called *the modular group*, and it has usually no geometrical interpretation, except in certain cases, the most famous example being the Rindler wedge in Minkowski space. In this case, the modular Hamiltonian is just the Boost generator, equal to the natural

Hamiltonian in the Rindler wedge. This is known as the Bisognano-Wichmann theorem [49, 50]. With this result in mind Ref [48] show that the modular flow just acts as a time shift in the hyperbolic frame. Specifically it is shown that

$$\tau \to \tau + 2\pi R s \tag{3.60}$$

and so the Hamiltonian is given by $H_{\mathcal{R}} = 2\pi R H_\tau + \log Z$.

The conformal then map sends the entanglement density matrix on $\mathcal{D}(\mathbf{B}^n)$ into the thermal density matrix of the hyperbolic space-time, with $T = 1/2\pi$, in units of the radius of curvature. The only feature that remain to be shown is that the transformation 3.60 is a symmetry of the correlators. If the correlation functions are defined for scaling operators of conformal dimension Δ_i we have

$$\langle\, \mathcal{O}_1(y_1) \cdots \mathcal{O}_s(y_s) \,\rangle_{\beta,\, \mathbf{H}^n} = \Omega(y_1)^{\Delta_1} \cdots \Omega(y_s)^{\Delta_s} \,\langle\, \bar{\mathcal{O}}_1(\bar{y}_1) \cdots \bar{\mathcal{O}}_s(\bar{y}_s) \,\rangle_{vac,\, \mathcal{D}(\mathbf{B}^n)} \tag{3.61}$$

where the operators $\mathcal{O}(y)$ at points $y \in \mathbf{R} \times \mathbf{H}^n$ are the images under the conformal map of the operators $\bar{\mathcal{O}}(\bar{y})$ at points $\bar{y} \in \mathcal{D}(\mathbf{B}^n)$. Under the imaginary time shift 3.60, one can check that the different factors coming from the conformal transformation and the correlators in $\mathcal{D}(\mathbf{B}^n)$ cancel each other, leaving the correlator in the hyperbolic manifold invariant.

With these insights at hand, consider now the retarded two-point function of an operator $\bar{\mathcal{O}}(\bar{y}) = \bar{\mathcal{O}}_{\Delta(\bar{t},\bar{x})}$ in the Minkowski vacuum of the CFT. We may write it as the imaginary part of the time-ordered correlation function, i.e.

$$\bar{G}_{ret}(\bar{t},\bar{x}) \propto \theta(-\bar{t}\,) \cdot Im\, \left\langle\, T\left[\bar{\mathcal{O}}_\Delta(0,0)\, \bar{\mathcal{O}}_\Delta(\bar{t},\bar{x})\right] \right\rangle_{vac,\, \mathcal{D}} = Im\, \frac{\theta(-\bar{t}\,)}{(-\bar{t}^{\,2} + |\bar{x}|^2 + i\,0)^\Delta}\,, \tag{3.62}$$

where $\theta(t)$ is the Heaviside function and we have used conformal invariance in the last step. Since we assume the CFT to be unitary, Δ is real, and the retarded correlation function is a distribution supported on the Minkowski (past) light cone of the origin, $\bar{t}^{\,2} = |\bar{x}|^2$, $\bar{t} < 0$, just like it was for free fields. Applying now the conformal map (3.61) we learn that the *thermal* retarded Green function on the hyperbolic manifold

$$G_{ret}(t,x) = \Omega(t,x)^{\Delta}\, \Omega(0,0)^{\Delta}\, \bar{G}_{ret}(\bar{t},\bar{x}) \tag{3.63}$$

is supported on the image of the light-cone under the conformal map. The conformal transformations send light-cones into light-cones, so that $G_{ret}(t,x)$ is supported on the past light-cone of the origin in $\mathbf{R} \times \mathbf{H}^n$. This proves that the fully interacting Green function in the hyperbolic space-time is supported on the light-cone, and thus any diffusion poles (for $\mathcal{O}_\Delta(y)$ equal to a conserved current of dimension $\Delta = n$) must be compatible with the ballistic propagation on the hyperboloid.

It would be interesting to prove the ballistic character of thermal Green functions directly for discrete quantum systems on finite expander graphs. Perhaps such a proof can be approached by first solving the intermediate case of the Bethe lattice, a discrete expanding geometry of infinite volume.

Chapter 4

The Streched Horizon as a Fast Scrambler

In the past chapter a scrambling framework has been developed without any mention to Black Hole Physics. In this chapter we are going to deal in detail with these intriguing objects from this perspective.

The objective is to develop a theory of information diffusion in Black Holes and/or SH, and abstract its typical time scales, with special emphasis on the scrambling time scale.

The chapter is organized as follows. The first section points out a universal structure characterizing non-extremal events horizons. In particular it shows the appearance of an hyperbolic space, as the *optical metric* of the near horizon region of every thermal horizon. In the second section it is shown how this optical metric naturally defines the concept of *Streched Horizon*, as the limit of applicability of Low Energy Field Theory, LEFT, in the renormalization group sense. In view of these facts, and using the results of the past two chapters, we propose two models of Information Scrambling in the vicinities of Black Hole Horizons, depending on the coupling regime of the LEFT.

The last section steps on these past constructions to abstract a putative theory of information diffusion in the Planckian Streched Horizon. The hyperbolic nature of the near horizon naturally selects an *ultrametric* theory with specific transition amplitudes, saturating stability bounds for the diffusion process. It is shown that this theory is again a Fast Scrambler.

4.1 The Hyperbolic Optical Metric

The diversity of thermal horizons in String Theory is certainly vast. It would be interesting to have certain common structure from which to look them all. In the case of extremal black holes, and more generically extremal black branes, this structure turns out to be AdS space with all its insightful implications, beautifully unified in the AdS/CFT correspondence. In the non-extremal case it is proposed that the universal structure is $\mathbf{R} \times \mathbf{H}^n$, which appears as the universal optical metric of thermal horizons [1]. This section shows that this is indeed the case for a vast class of thermal horizons.

4.1.1 Rindler, de Sitter and Hyperbolic space-times

We begin with Rindler and de Sitter space-times, which are basically trivial to analyse in this regard, and for which the conformal map is exact in the whole space.

The first and basic observation of all our approach to Black Hole information scrambling is the conformal optical map between $\mathbf{R} \times \mathbf{H}^n$ and Rindler space-time, with metric

$$ds^2_{\text{Rin}} = -y^2 dt^2 + dy^2 + d\ell^2 \ , \tag{4.1}$$

where the ℓ coordinates parametrize $\mathbf{R}^{n-1}$. The optical frame then yields $\mathbf{R} \times \mathbf{H}^n$, presented in the upper-half plane coordinates

$$ds^2_{\widetilde{\text{Rin}}} = -dt^2 + \frac{dy^2 + d\ell^2}{y^2} \ . \tag{4.2}$$

In a similar way there is a global conformal map between the space $\mathbf{R} \times \mathbf{H}^n$ and the static patch of de Sitter space-time, dS_{n+1}, which is the patch covered by the cosmological horizon with metric

$$ds^2_{\text{dS}} = (1-u^2)\, dt^2 + (1-u^2)^{-1} du^2 + u^2\, d\Omega^2_{n-1} \ . \tag{4.3}$$

The corresponding optical frame is given by

[1] The so-called optical metric is obtained by removing the $|g_{00}|$ factor in any static metric by a conformal transformation (cf. for example [46] for a recent review)

$$ds^2_{\widetilde{\mathrm{dS}}} = -dt^2 + \frac{du^2}{(1-u^2)^2} + \frac{u^2}{(1-u^2)}\, d\Omega^2_{n-1} = -dt^2 + dr^2 + (\sinh r)^2\, d\Omega^2_{n-1}\ , \tag{4.4}$$

which is again globally identical to $\mathbf{R}\times\mathbf{H}^n$, this time in global coordinates, under the coordinate change $\sinh r = u(1-u^2)^{-1/2}$.

4.1.2 Black Branes

Here we show this interesting feature for Black Branes, living in a $\mathbf{X}^{d+2}$ spacetime, like the ones consider in chapter 2 (2.1), when computing the free fall time.

To see this, notice that near a regular, static horizon we may choose $(d+2)$-dimensional coordinates exhibiting a two-dimensional Rindler factor in the near-horizon geometry $\mathbf{X}^{d+2}$, of the form

$$ds^2_{\mathbf{X}} = g_{\mu\nu}\, dx^\mu dx^\nu \approx F(\rho, y)\left(-\left(\frac{2\pi\rho}{\beta}\right)^2 dt^2 + d\rho^2\right) + H_{ij}(\rho, y)\, dy^i\, dy^j\ , \tag{4.5}$$

where the horizon is conventionally located at $\rho = 0$. The functions $F(\rho, y)$ and $H_{ij}(\rho, y)$ are assumed to have smooth expansions around $\rho = 0$, as is the case for the *holographic* branes 2.1.

The optical manifold $\widetilde{\mathbf{X}}$ is defined in the exterior region $\rho > 0$ through the conformal transformation

$$ds^2_{\mathbf{X}} = \Omega^2(\rho, y)\, ds^2_{\widetilde{\mathbf{X}}}\ , \qquad \Omega(\rho, y) = \frac{2\pi\rho}{\beta}\sqrt{F(\rho, y)}\ , \tag{4.6}$$

with near-horizon asymptotic form

$$ds^2_{\widetilde{\mathbf{X}}} \approx -dt^2 + dz^2 + e^{4\pi z/\beta}\, \gamma_{ij}(y)\, dy^i dy^j\ , \tag{4.7}$$

where $\gamma_{ij} = (H_{ij}/F)_{\rho=0} + \mathcal{O}(\rho^2)$, and we have defined a Regge–Wheeler or 'tortoise' radial coordinate $\rho = e^{-2\pi z/\beta}$, in terms of which the Rindler region extends roughly along the interval $z \in [0, \infty]$, with the horizon sitting at $z = \infty$.

Up to terms exponentially suppressed at large z, the near-horizon optical metric is 'asymptotically locally hyperbolic', with obvious 'z-expanding' properties in the sense of the last section. The spatial

metric $d\ell^2 = \gamma_{ij}\, dy^i dy^j$ is induced at the edge of the Rindler region, and it is related to the physical induced metric at the horizon by a regular conformal transformation. Since γ_{ij} defines a conformal compactification of the horizon boundary, the obvious analogy with the AdS/CFT correspondence was exploited in Ref. [51] to propose a dual Euclidean CFT description on the γ-geometry. In this paper, we take a different route and emphasize the relation between (4.7) and microscopic models of the stretched horizon.

It is also interesting to obtain the optical metric in the asymptotic region of the Black Brane metrics 2.1. This is represented by a flat strip of length β,

$$ds^2_{\tilde{\mathbf{x}}} \approx -dt^2 + dz^2 + d\ell^2 \,, \qquad 0 < z < z_\beta \sim \beta \,, \tag{4.8}$$

with optical depth of order $z_\beta \sim \beta$. It is remarkable that, despite the non-AdS nature of the asymptotic regions, the optical metric is still given by 4.8 for all Dp-brane throats with $p < 5$, including the fact that the optical distance to infinity is given by the inverse temperature β.

This observation helps us understand why the free fall time is controlling the fast spreading of charges at the Streched Horizon, described in chapter 1. This is particularly clear in the optical representation of the thermal cell depicted in Figure 4.1. The whole non-compact asymptotic region is mapped to a small box of size β, so that induced charges at the stretched horizon are quite insensitive to the motion of source charges in the asymptotic region. The optical metric is dominated by the near-horizon region, and the time-scale for global causal communication across this region defines the time scale for large-scale rearrangements of induced charges at the stretched horizon (notice that Maxwell's equations are conformally invariant, so that electromagnetic field solutions can be faithfully studied in the optical frame).

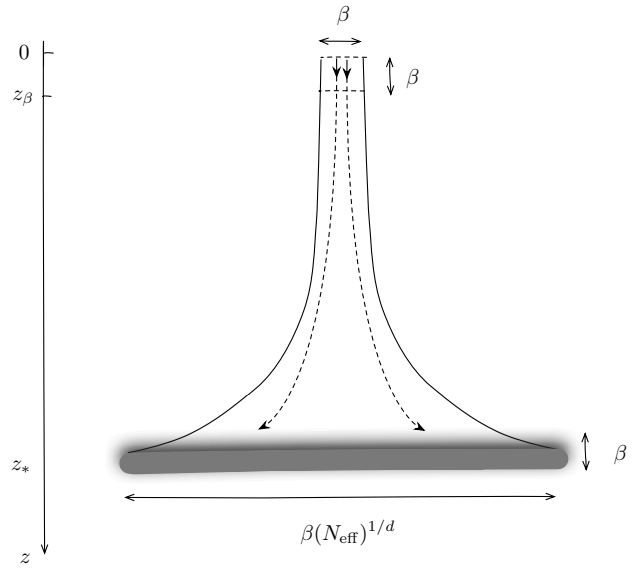

Figure 4.1: The optical box of a single thermal cell of CFT volume β^d, drawn to indicate the optical-volume expansion of the spatial sections up to an optical volume N_{eff} times larger at the stretched horizon, itself with optical thickness of $\mathcal{C}O(\beta)$. The vacuum piece $z \ll z_\beta$ has negligible optical volume compared to the Rindler piece $z_\beta \ll z \ll z_*$, which dominates the AdS/CFT computation of any boundary observable in the long-time limit. Exponential sensitivity to initial conditions in the UV leads to chaotic classical behavior in the near-horizon region.

4.2 The optical *Strech*

In this section we explain why the optical metric is a useful tool in any discussion of near-horizon dynamics. Any such description involves a finite number of local fields with Hartle–Hawking boundary conditions at $\rho = 0$, which are equivalent to the specification of a thermal state at locally measured temperature $(\beta\sqrt{-g_{00}})^{-1}$. Let us parametrize the effective action of any such LEFT in the schematic form (here for a scalar field degree of freedom Ψ)

$$S_{LEFT} = -\int_{\mathbf{X}^{d+2}} \left[\tfrac{1}{2}\Psi \left(-\nabla^2_{\mathbf{X}} + \frac{d}{4(d+1)} R[\,\mathbf{X}\,] + M^2 \right) \Psi + \sum_{\mathrm{i}rr\ \mathcal{O}} \frac{\lambda}{\Lambda^{\Delta-d-2}} \mathcal{O}(\Psi) \right] . \tag{4.9}$$

In this expression, the Laplacian has been corrected by a conformal coupling to the Ricci-scalar $R[\mathbf{X}]$, so that the remaining terms give the strength of conformal symmetry breaking. M is a typical mass, standing as a representative of whatever relevant operators we may have turned on, and the remaining sum accounts for characteristic irrelevant operators with conformal weight $\Delta > d+2$, dimensionless coupling λ and scale Λ, playing the role of Wilsonian UV cutoff for the LEFT.[2] Consistency of the Wilsonian procedure requires $M < \Lambda$. Since the Hartle–Hawking quantum state to be stored on the fields Ψ has energy scale $1/\beta$, the Wilsonian consistency also requires the constraint $1/\beta < \Lambda$.

At this point we are free to perform field redefinitions in (4.9) if they serve the purpose of illustrating the physics, just as it is sometimes natural to switch back and forth between so-called Einstein and string-frames in the graviton-dilaton system arising in low-energy string-theory Lagrangians. In the same vein, we shall rewrite (4.9) in the 'optical' frame, together with the field redefinition

$$\Psi = \Omega^{-d/2}\, \widetilde{\Psi} \ . \tag{4.10}$$

Using the identity

$$\left(-\nabla^2_{\mathbf{X}} + \frac{d}{4(d+1)} R[\,\mathbf{X}\,] \right) \Omega^{-d/2} = \Omega^{-2-d/2} \left(-\nabla^2_{\widetilde{\mathbf{X}}} + \frac{d}{4(d+1)} R[\,\widetilde{\mathbf{X}}\,] \right) , \tag{4.11}$$

we finally obtain

$$S_{LEFT} = -\int_{\widetilde{\mathbf{X}}^{d+2}} \left[\tfrac{1}{2}\widetilde{\Psi} \left(-\nabla^2_{\widetilde{\mathbf{X}}} + \frac{d}{4(d+1)} R[\,\widetilde{\mathbf{X}}\,] + M^2_{eff} \right) \widetilde{\Psi} + \sum_{\mathrm{i}rr\ \mathcal{O}} \frac{\lambda}{(\Lambda_{eff})^{\Delta-d-2}} \mathcal{O}(\widetilde{\Psi}) \right] . \tag{4.12}$$

[2] We adopt the 'naturality' convention in which the strength of the coupling is controlled by Λ, i.e. $\lambda = \mathcal{O}(1)$.

The result is a conformally-invariant effective action, perturbed by relevant and irrelevant operators with effective position-dependent dimension-full parameters $M_{eff}(z) = \Omega(z)M$ and $\Lambda_{eff}(z) = \Omega(z)\Lambda$. Since $\Omega(z \to \infty) \to 0$, all these dimension-full parameters are scaled to zero in the horizon limit. Hence, the $z \to \infty$ limit is a zoom into the UV structure of the LEFT, isolating the conformally-invariant dynamics of whatever field degrees of freedom exist below the Wilsonian cutoff Λ, while at the same time blowing up the irrelevant operators heralding the approach to the UV cutoff.[3] Since the thermal state of interest has scale $1/\beta$, the running of the effective dimensionless coupling of irrelevant operators, defined at scale $1/\beta$, is given by

$$\lambda_{eff}(z) = \frac{\lambda}{(\beta\Lambda\Omega(z))^{\Delta-d-2}} \ . \tag{4.13}$$

Since $\lambda = \mathcal{O}(1)$, the effective position-dependent coupling enters strong-coupling at the point z_Λ determined by

$$\Omega(z_\Lambda)\Lambda = 1/\beta \ . \tag{4.14}$$

Therefore, $z = z_\Lambda$ marks the end of the LEFT domain of applicability, and thus defines the edge of the Λ-*stretched* horizon. We see then how the optical metric naturally defines de concept of a SH by the blowing up of irrelevant operators in the renormalization group sense. In general, in the context of 'black hole complementarity' [19], we shall define the SH as the limit of applicability of Low-Energy-Field-Theory (LEFT). The minimal choice for Λ is then of the order of the Planck mass, $M_{\rm P}$, defining the standard notion of a Planckian stretched horizon at the corresponding solution $z_{\rm P}$ of (4.14), but other choices are possible. Consider for example a perturbative string theory with string mass scale M_s, which defines a stringy stretched horizon at optical depth z_s. In general we have $\Lambda = M_s = {g_s}^{\alpha} M_{\rm P}$ with $g_s \leq 1$ the string coupling and $\alpha > 0$. Solving the equations $1/\beta = \Omega(z_s)M_s = \Omega(z_{\rm P})M_{\rm P}$ yields the optical depth difference

[3]The conformal mass term is *n*egative, approaching $-(\pi\, d/\beta)^2$ as $z \to \infty$. Since the $\widetilde{\mathbf{X}}$-Laplacian is gapped in the same amount, only the zero mode of $\widetilde{\Psi}$ is tachyonic. This mode is seriously non-normalizable in the original $\mathbf{X}$-frame field Ψ, so it does not satisfy the Hartle–Hawking boundary conditions and should be treated as non-dynamical in the LEFT.

$$z_{\rm P} - z_s = \frac{\beta}{2\pi} \log\left(\frac{M_{\rm P}}{M_s}\right) = \frac{\beta}{2\pi}\, \log(1/g_s^\alpha)\ . \tag{4.15}$$

In this case, despite the fact that the string theory remains weakly coupled at $z \sim z_s$, the effective mass of the whole Hagedorn tower of massive string states comes down below the $1/\beta$ scale as $z < z_s$. Therefore, the dynamics is expected to become non-perturbative because of the exponential growth of field species.

Another interesting case is that of a 'thick' stretched horizon, arising for $\Lambda \sim 1/\beta$, i.e. a situation where there is essentially no LEFT description at all. This corresponds to the bulk dynamics of holographic gauge theory duals with 't Hooft coupling of $\mathcal{O}(1)$. Such models are akin to large-N, weakly coupled matrix models with possibly complicated interactions.

We notice here that the free fall time discussed in chapter 2 translates in the optical metric to the size of this *cut-off* hyperbolic space. Therefore we call this scale the optical depth, the size of the optical metric. As we saw in the second chapter, this optical depth is of the same order of the conjectured scrambling time scale, a fact that would be crucial in the scrambling models to be defined below.

The physics of (4.9) in the radial domain $0 \ll z \ll z_\Lambda$, deep within the Rindler region but still clear from the stretched horizon, consists of a conformal thermal state. [4] Since the optical metric is ultra-static, the thermodynamic functions of such a thermal state are extensive on the hyperbolic spatial geometry. For example, the entropy of Ψ-field states contained in Rindler, up to optical depth z, scales with the optical volume

$$S_\Psi \sim \widetilde{V}_z\, \beta^{-d-1}\ , \tag{4.16}$$

where

$$\widetilde{V}_z = V \int_0^z dz'\, e^{2\pi z' d/\beta} \approx V\, \frac{e^{2\pi z d/\beta}}{2\pi d}\ , \tag{4.17}$$

and $V \equiv V_\gamma$ is the volume in the γ_{ij} metric. Hence, we have a uniform excitation density of $\mathcal{O}(1)$ degrees of freedom per thermal

[4] The discussion leading to (4.9) generalizes to any non-trivial CFT perturbed by relevant and irrelevant operators with respective scales M and Λ.

volume β^{d+1} of optical bulk, although the 'expanding' nature of the geometry forces all extensive quantities to become dominated by the large z-cutoff (states pile up in the last layer of $\mathcal{O}(\beta)$ thickness). The old result of 't Hooft's brick-wall model [52,53] follows in this language as the (approximate) matching of the entropy in sub-Planck Hawking radiation with the Bekenstein–Hawking entropy of the black hole:

$$S_{\mathrm{B}H} \sim \widetilde{V}_{z_{\mathrm{P}}}\, \beta^{-d-1}\ . \tag{4.18}$$

Again, this entropy is roughly accounted for by the last layer of optical thickness of $\mathcal{O}(\beta)$ (equivalently $\mathcal{O}(\ell_{\mathrm{P}})$ thickness in the physical metric).

4.3 Horizon scrambling models

In this section all the data from previous sections and chapters is used to propose three models of information scrambling in Black Hole spacetimes. They all will naturally appear to be Fast scramblers. They do not mean to be incompatible and the three mechanisms that we propose may be well working at the very same time. All together they furnish a theory of information processing at thermal horizons, to be contrasted with the dual Matrix Models.

4.3.1 Expander diffusion

The first model considers the possibility of a putative stringy Black Hole, dual of a large N gauge theory at small t'Hooft coupling. In this regime, as commented before, we expect strong coupled dynamics in the whole near horizon region. In other words, the Λ-stretched horizon covers all the thermal atmosphere.

We will now make a basic assumption regarding the structure of this Λ-stretched horizon. We declare that the geometrical structure of $\widetilde{\mathbf{X}}$ is still relevant to characterize the interactions of strongly-coupled degrees of freedom building up this region. More precisely, we model the stretched horizon as an effective hyperbolic lattice of $\mathcal{O}(\beta)$ spacing with a worth of $\mathcal{O}(1)$ Q-bit degrees of freedom per lattice point. In other words, we have a strongly-coupled discrete quantum system on a cut-off expander graph.

The dimension of this Hilbert space is fixed by the matching to the Bekenstein–Hawking entropy. In particular, we have the extensive behaviour (4.16), now applying to the dimension of the Hilbert space, rather than simply the entropy of excitations:

$$\log \mathrm{d}im\, \mathcal{H}_{\mathrm{S}H} \sim \widetilde{V}_{\mathrm{S}H}\, \beta^{-d-1} \sim S_{\mathrm{BH}} \ , \tag{4.19}$$

where $\widetilde{V}_{\mathrm{S}H} \sim \widetilde{V}_{z_{\mathrm{P}}}$ and we have used (4.18).

Setting $V = V_\gamma = \beta^{\,d}$, we deal with a single thermal cell, and the associated entropy is just the specific entropy $S_{eff} = S_{cell} = N$. Inverting (4.17) we find the relation between the maximal depth of the stretched horizon and the specific entropy

$$z_{\mathrm{P}} = \frac{\beta}{2\pi d}\, \log\, N \ , \tag{4.20}$$

for the total optical depth at the 'bottom' of the stretched horizon.

At this point, we can make contact with the discussion in section 2, characterizing horizon scrambling in terms of a discrete diffusion process with step β, playing on the expander graph cutoff to depths $z_\Lambda < z < z_{\mathrm{P}}$. The expander-diffusion process scrambles $\mathcal{O}(n)$ degrees of freedom of a single thermal cell in a time of order $\beta \log(n)$, as the random walk reaches the 'bottom' of the stretched horizon at $z = z_{\mathrm{P}}$.

Now, in a first approximation [5], any subsequent scrambling over scales larger than a thermal cell of the γ_{ij} metric proceeds by standard diffusion on the 'bottom' of the expander with induced (optical) metric

$$d\ell^2_{z_{\mathrm{P}}} = e^{4\pi\, z_{\mathrm{P}}/\beta}\, \gamma_{ij}\, dy^i dy^j = N^{2/d}\, \gamma_{ij}\, dy^i dy^j \ . \tag{4.21}$$

Hence, a length scale $L \gg \beta$ in the γ_{ij} metric corresponds to a length scale $L\, N^{1/d} \sim (NV)^{1/d}$ in the bottom metric (4.21). Such a patch is slow-scrambled in a time of order $\beta^{-1}\, (VN)^{2/d}$. The number of thermal cells on the patch is V/β^d. Since N is the entropy per thermal cell we may write the total entropy of the patch as $S \sim N\, V\, \beta^{-d}$, so that the total slow-scrambling time is the standard diffusive $\beta\, S^{\,2/d}$ result. It is important to notice that this result is non-trivial, since it

[5] We will provide a different diffusion model in the next section more suited for the dynamics of a single thermal cell. In any case, the results for the scrambling time in spatial domains larger than a thermal cell is unchanged because this new diffusion model will only operate again at the level of one cell.

has been derived for systems which have $\mathcal{O}(N)$ degrees of freedom per thermal cell, rather than $\mathcal{O}(1)$ degrees of freedom as in the common case.

Combining these estimates we finally find the fast-scrambling law

$$\tau_s(L) \sim \beta \log N \,, \qquad L \leq \beta \tag{4.22}$$

below the thermal cell scale, and the slow-scrambling law

$$\tau_s(L) \sim \beta \, S^{2/d} \,, \qquad L \gg \beta \tag{4.23}$$

for distances well above the thermal cell.

The estimate (4.23) is quite general, since it only depends on the bottom density of the expander. On the other hand, (4.22) assumes tacitly that the expander graph starts at $z = z_\Lambda \sim 0$, i.e. the stretched horizon covers the whole Rindler region. Such a situation is only appropriate for highly stringy black holes dual to weakly-coupled CFTs, as commented at the beginning of this section. Smooth horizons with a large Rindler region where LEFT is valid support 'thin' stretched horizons for which the fast-scrambling diffusion operates for a smaller time of order $\beta \log(N) - z_\Lambda$. In particular, in the limit in which we push the LEFT validity down to Planckian distances from the horizon, we have $z_\Lambda \sim z_{\rm P}$ up to $\mathcal{O}(1)$ factors, and the optical thickness of the Λ-*stretched* horizon is only of $\mathcal{O}(\beta)$. In such a situation the random walk diffusion is always slow-scrambling in a first naive approximation.

However, as we develop in the next section, surface-scattering effects may affect this picture.

4.3.2 Chaotic billiard

The last commentaries of the past subsection lead us to the second scrambling model, the Chaotic billiard [1].

We suppose a weakly coupled bulk theory, dual to some gauge theory at large t'Hooft coupling. In this regard we neglect the collisions of $\mathcal{O}(1/N_{eff})$ strength within the bulk of the thermal atmosphere. The near horizon optical region is a weakly coupled hyperbolic field theory in the thermal state, which can be approximated as an ideal gas.

Within this setup we consider a Planck-localized probe following null geodesics in the Rindler region, punctuated by collisions of $\mathcal{O}(1)$

strength at the stretched horizon. These collisions cannot be avoided, as described in the past section. In order to benefit from the geometrical intuition, we notice that any such piecewise-null trajectory defines a corresponding piecewise-null trajectory on the conformally-related optical manifold (4.7) with hyperbolic spatial sections. Therefore, we can use the optical metric to discuss the dynamical time scales of such an ideal probe motion. The advantage of this description is the uniform proportionality between time scales for null propagation and 'optical' length scales, together with the simplicity of hyperbolic geodesics.

Consider then a localized probe sent radially inwards with a maximal (Planck) bulk resolution at the top of the Rindler region, as measured in the physical metric (2.1), i.e. the initial resolution $\delta\ell_i$ in the ℓ coordinate satisfies

$$F_0\,(\delta\ell_i)^2 \sim \ell_{\rm P}^2\ . \tag{4.24}$$

The geometrical stretching of the optical metric implies that such a probe is smeared over a region whose optical size in the ℓ directions is of order

$$\delta s_{op} \sim \frac{\delta\ell_i}{\sqrt{h_*}} \sim \frac{\ell_{\rm P}}{\sqrt{F_0 h_*}} \sim \beta \tag{4.25}$$

on arrival to the stretched horizon. The thermal state of strongly interacting degrees of freedom at the stretched horizon has thermal length of $\mathcal{O}(\beta)$ (again, in the optical metric), which determines the effective interaction length of probe scattering at the stretched horizon. Since the effective resolution in the impact parameter for these scattering events is also of $\mathcal{O}(\beta)$, we conclude that the outgoing scattering angle at each collision has maximal uncertainty.

In between scattering events the probe is assumed to glide freely on the Rindler region. Maximizing the glide velocity, we can assimilate the motion to a random walk on a $(d+1)$-dimensional hyperboloid with steps made of geodesic arcs on the spatial sections of the optical geometry:

$$ds_{op}^2 \approx -dt^2 + \left(\frac{\beta}{2\pi}\right)^2 \frac{dy^2 + d\ell^2}{y^2}\ . \tag{4.26}$$

In the Poincaré coordinates of (4.26), each free glide between collisions is a circular arc with radius $\Delta y \sim \Delta\ell/2$ if the collision points are separated a distance $\Delta\ell$ in the QFT metric (cf. Figure 2). The maximum extent of a circular glide is given by arcs of radius $y_{max} \sim \beta$. The reason is that the scarce[6] trajectories with larger radii hit the end of the Rindler region and are effectively reflected back by the confining wall of the asymptotic AdS region, the resulting complete trajectory returning to the stretched horizon at $\Delta\ell < \beta$. We thus conclude that, after a few scattering events, there is complete uncertainty about the position of the probe within a distance scale of the order of the QFT thermal length. Since each maximal glide through the optical hyperboloid takes a time of $\mathcal{O}(\tau_*)$, we conclude that the 'position' scrambling of the Planckian probe within the thermal cell has been achieved in times of order $\tau_* \sim \beta \log(S_{cell})$. This is shown schematically in Figure 4.2.

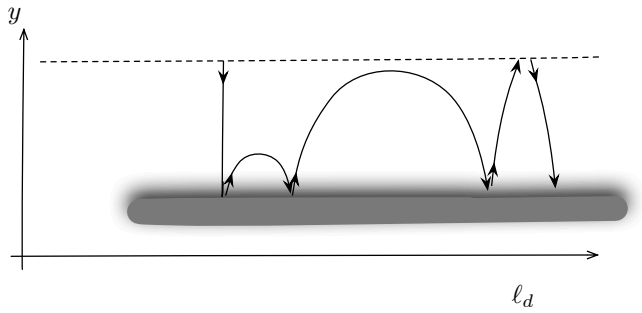

Figure 4.2: Near-horizon random walk of a localized probe by scattering at the stretched horizon, pictured in the Poincaré coordinates of the spatial optical metric (4.26). Free paths between successive collisions are circular arcs, with maximal radius $\Delta y_{max} \sim \beta$, since longer glides are reflected back by the asymptotic AdS potential well which starts at the edge of the Rindler region, represented in this picture by a dashed line.

The kinetic model presented here regards the near-horizon region as a chaotic billiard over a negative-curvature space, one of the early examples of hard chaos in classical mechanics [54, 55]. Indeed, if we

[6]The proportion of solid angle enclosing those trajectories which are 'vertical' enough to hit the end of the Rindler region is of the order of $\delta^d/\mathrm{V}ol(\mathbf{S}^d) \sim (h_*)^{d/2} \sim 1/N_{eff}$.

substitute the stretched horizon by a random arrangement of hard reflecting spheres of size β in the optical metric, we get essentially the same picture. The Lyapunov exponent, defined locally in terms of the divergence rate of geodesics, is of order $\lambda_{\rm L} \sim \beta^{-1}$. The Lyapunov time, defined as the time for complete erasure of localization information, from an initial resolution $\delta\ell_i$ to a final resolution of one thermal length $\delta\ell_f \sim \beta$, is of order

$$\tau_{\rm L} \sim \lambda_{\rm L}^{-1} \log(\delta\ell_i/\delta\ell_f) \sim \beta \, \log(\ell_{\rm P}/\beta\sqrt{F_0}) \sim \tau_* \, , \tag{4.27}$$

since complete ignorance over the position of the Planck-size probe on the extent of a thermal cell is achieved after $\mathcal{O}(1)$ collisions, with characteristic collision time of $\mathcal{O}(\tau_*)$.

Our proposed 'ballistic catalysis' of the scrambling is only effective as long as the glides are large geodesic arcs on the hyperbolic optical geometry (4.26). Since the finite extent of the Rindler region imposes an effective cutoff to the size of these arcs, on time scales larger than τ_* the system behaves as a slow scrambler with effective time step τ_*. This is again the same insight as in the past model, which show that Fast Scramblers must be *small*.

Therefore, the whole system with n_{cell} thermal cells is scrambled in a time $\tau_s \sim \tau_*(n_{cell})^{2/d}$. In other words, the scrambling time of a general horizon as a function of the entropy and the effective number of degrees of freedom is shown to be

$$\tau_s \sim \beta \, \log(N_{eff}) \, (n_{cell})^{2/d} \sim \beta \, \log(N_{eff}) \, \left(\frac{S}{N_{\rm e}ff}\right)^{2/d} \, . \tag{4.28}$$

More generically, we can expect the combined effect of classical chaos, with $\mathcal{O}(1)$ 'atmospheric' collision events, and the standard diffusion upon absorption by the expander graph, altogether accounting for the expected scrambling properties of idealized probes. A cartoon of this picture is offered in figure 4.3.

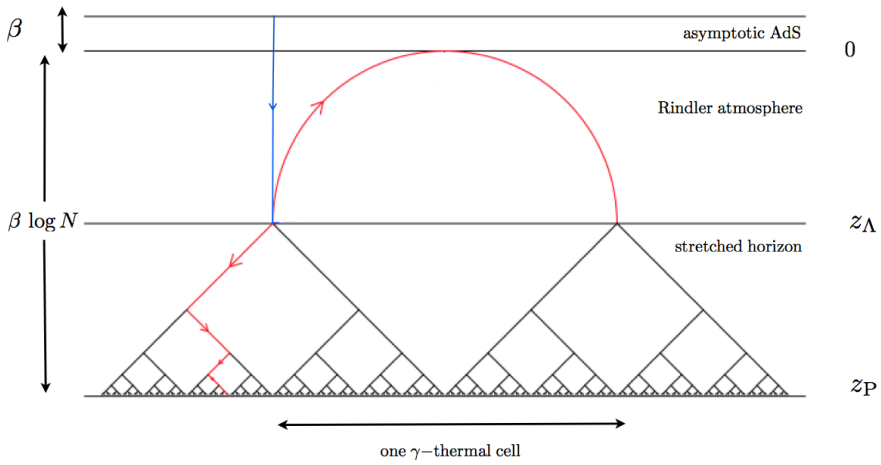

Figure 4.3: Schematic view of the effective kinetic scrambling model in the optical frame, featuring a Cayley tree picture of the stretched horizon, a hyperbolic 'Rindler atmosphere' and an asymptotic AdS region of optical depth of $\mathcal{O}(\beta)$. The total optical depth of the hyperbolic section $[0, z_P]$ is $\mathcal{O}(\beta \log N)$. A localized classical probe injected from the asymptotic boundary (vertical blue line) is either absorbed or reflected at $z = z_\Lambda$. If reflected (curved red line), it scrambles fast in the effective chaotic billiard of the Rindler atmosphere. If absorbed (jagged red line), it scrambles fast by diffusion on the expander graph until it reaches the bottom at z_P. Once at the bottom, it scrambles slowly by diffusion on the bottom. The fast-scrambling patch measured by the γ_{ij} metric is always about one thermal cell.

4.3.3 Ultrametric streched horizons

Phenomenological models based on propagation on hyperbolic geometry have the drawback of requiring rather strong assumptions on the dynamics of the whole near-horizon region (comprising the SH plus its 'thermal atmosphere'.) We either need a strongly interacting near-horizon region to set up a random walk on an expander graph, or a sufficiently stable probe must be assumed to justify the model of chaotic elastic scattering off the SH.

At the same time, the principle of Black Hole Complementarity

states that Black Hole dynamics should be completely described by LEFT together with Streched Horizon dynamics. Despite intensive study, the detailed structure of SHs remains mysterious beyond these very general thermodynamical and hydrodynamical considerations. One important point of contention is the status of locality of the effective SH Hamiltonian. Although the count of degrees of freedom may suggest a local system with Planckian cutoff, there are various reasons to suspect that a highly non-local dynamics is at play. After all, if the SH is defined as the dynamics which cannot be described by low-energy QFT in the bulk, it is natural to assume that this dynamics will be in conflict with at least one of the two cornerstones of low-energy QFT: unitarity and locality, the second one being the obvious choice.

In this section we advance in this picture, and try to combine the virtues of both previous models. We shall continue to model scrambling in terms of discrete classical diffusion, but remove the assumption of locality. At the same time, we require the non-local diffusion kernel to just saturate the causality requirements, without sacrificing stability bounds. One way of representing these conditions is to regard the SH as the boundary of a cut-off expander graph, and then 'integrate out' the bulk of the expander graph, retaining only the transition amplitudes between points on the boundary. Since, as described in chapter 3, expander graphs are well-approximated by regular trees, we can simplify matters by considering a Cayley tree of fixed branching rate $d+1$, which provides a discretization of a hyperbolic geometry in $d+1$ dimensions.

A single thermal cell of the SH will be modeled by S points over which we define a positive probability density, undergoing discrete diffusion as specified by the equation

$$\partial_t \rho = W \rho \,, \tag{4.29}$$

where ρ is a S-vector and W is a $S \times S$ matrix of transition rates. Off-diagonal elements must then be positive,

$$W_{ij} \geq 0 \,, \quad i \neq j \tag{4.30}$$

and normalization $\sum_i \rho_i = 1$ determines the (negative) diagonal elements to be

$$W_{ii} = -\sum_{j \neq i} W_{ij} \ . \tag{4.31}$$

The crucial hypothesis on the matrix W_{ij} is the requirement that the individual rates W_{ij} between two points i and j of the SH be determined by the inverse of their causal time separation t_{ij}, where the causal times are computed as the times-of-flight of photons across the thermal atmosphere

$$W_{ij} \propto \frac{1}{t_{ij}} \sim \frac{1}{z_{ij}} \ . \tag{4.32}$$

Here z_{ij} denotes the discretized version of the tortoise coordinate for the turning point of a null geodesic joining points i and j. Since we model the hyperbolic geometry by a tree, the z coordinate is to be equated to the branching level n of the tree, measured from the SH, in units of the inverse Hawking temperature.

We stress that the nodes of the tree are *n*ot part of the SH, nor is the diffusion process 4.29 'playing out' on the tree. Rather, the tree is just used as a geometrical encoding of the appropriate causal times t_{ij} between two points on the SH, and hence the value of the elementary transition rate W_{ij}.

We regard the points on the SH as the top leaves of an auxiliary b-branching tree with $b = d + 1$. Therefore, any point on the SH has a single ancestor at level n, which is shared among a total of p^n points in the SH. The elementary transition time between any such points sharing a common ancestor is taken to be proportional to the level n, and be equal for all points sharing the same ancestor, so that the rate only depends on n, giving the transition matrix a hierarchical structure with block-entries of value W_n determined by their separation from the main diagonal.

Such a hierarchical structure is characteristic of so-called *ultrametric* spaces, in which distances are defined by ancestry rules such as those implied by the regular tree specified here. More generally, an ultrametric structure is defined by the rule that, given three points defining three distances, the two smaller ones are always equal. This is in violation of the standard triangle inequality of metric spaces, and can always be modeled by defining distance in terms of an ancestry level on a tree (not necessarily a regular one).

The characteristic time scale for the variation of the local density also depends on the phase space of final states. In particular, the total probability to jump from site i to any other point connected through a level-n ancestor is

$$\sum_{j_n} W_{ij_n} = (d+1)^{n-1} W_n \equiv e^{-I_n} \ , \tag{4.33}$$

where we have defined an 'effective action' for the transition through level n, characterizing the effective 'barrier height'. It becomes natural to include the entropic factor $(d+1)^{n-1}$ in the relation between the characteristic time scales and the matrix of transition rates:

$$e^{-I_n} \sim \frac{1}{t_n} \sim \frac{1}{n} \ . \tag{4.34}$$

This expression is the main assumption of our model, stating that the effective action for elementary transitions has a particular dependence with the ultrametric distance between initial and final states:

$$I_n = \log\, n + constant \ , \tag{4.35}$$

with exactly unit coefficient in front of the logarithm.

The general solution to the diffusion problem 4.29 on ultrametric spaces is well known (see for example [56]) and has been intensely studied in the context of disordered media and spin glasses. The relevant information is encoded in the spectral properties of the transition kernel W_{ij}.

The completely scrambled state $\rho_i = 1/S$ is an eigenvector of W with vanishing eigenvalue, all the rest being negative-definite. We choose to parametrize them in terms of the opposite-sign quasi-normal frequencies Γ_r which are the eigenvalues of the negative kernel $-W_{ij}$ and read,

$$\Gamma_r = d \sum_{k=R-r+2}^{R} e^{-I_k} + (d+1)\, e^{-I_{R-r+1}} \ . \tag{4.36}$$

In this expression, the index r runs over all integers in the interval $0 \leq r \leq R$, where R stands for the effective maximal ultrametric distance between the S points of the SH under consideration, and

is determined by the relation $(d+1)^R = S$. The expression 4.36 degenerates for $r = 0, 1$, for which we have

$$\Gamma_0 = 0 \ , \qquad \Gamma_1 = (d+1)\, e^{-I_R} \ . \tag{4.37}$$

Notice that Γ_1 gives the leading quasi-normal frequency which, for the particular case of interest 4.35 is given by

$$\Gamma_1 = (d+1)\, e^{-I_R} \sim \frac{1}{\log\, S} \ , \tag{4.38}$$

up to coefficients of $\mathcal{O}(1)$. Being the smallest positive quasi-normal frequency, Γ_1 determines the time scale for exponential relaxation to the uniform distribution,

$$t_S \sim \frac{1}{\Gamma_1} \sim \log\, S \tag{4.39}$$

confirming that ultrametric diffusion with the particular barrier landscape 4.35 defines a *fast scrambler*.

A distribution of the form 4.35 has a special significance in the context of general ultrametric diffusion laws. In standard applications in the theory of disordered media one usually considers linearly growing landscapes, with a law of the form $I_n \propto n + constant$. These type of systems exhibit quite slow diffusion, interpolating between localization-type behavior and standard gaussian random walks. On the other hand, logarithmic landscapes with a barrier growth of the form

$$I_n = \alpha\, \log(n) + constant \tag{4.40}$$

lead to the so-called Kohlrausch-law behaviour, with a diffusion law that can be tuned to be *faster* than a gaussian random walk. An interesting quantity which is sensitive to the dynamical coefficient α in 4.40 is the return walk probability. Starting with an initial distribution completely localized at single origin point $i = o$, i.e. $\rho_i(0) = \delta_{io}$, we consider the return probability to the origin after time t, which can be written quite explicitly,

$$\rho_o(t) = \frac{1}{S} + \sum_{r=1}^{R} \frac{d}{(d+1)^{R-r+1}}\, e^{-\Gamma_r\, t} \ , \tag{4.41}$$

for the present case of a regular tree with branching $b = d + 1$.

For a landscape of the form 4.40 the spectrum of quasi-normal modes is

$$\Gamma_r/c = \frac{d+1}{(R-r+1)^\alpha} + d \sum_{k=R-r+2}^{R} \frac{1}{k^\alpha} = \frac{1}{(R-r+1)^\alpha} + d \sum_{k=R-r+1}^{R} \frac{1}{k^\alpha} \,, \tag{4.42}$$

where c is an overall proportionality constant of order $\mathcal{O}(1)$. If inserted back into 4.41, after relabeling the index sum we obtain

$$\rho_o(t) = \frac{1}{S} + \sum_{l=1}^{R} \frac{d}{(d+1)^l} \exp\left(-ct\left(\frac{1}{l^\alpha} + d\sum_{k=l}^{R}\frac{1}{k^\alpha}\right)\right) \,. \tag{4.43}$$

This expression shows that $\alpha = 1$ is a critical value for the stability of the random walk in the thermodynamical limit $R \sim \log S \to \infty$. For large R we may approximate the k-sum by

$$\sum_{k=l}^{R} \frac{1}{k^\alpha} \sim \frac{1}{\alpha - 1}\left(\frac{1}{l^{\alpha-1}} - \frac{1}{R^{\alpha-1}}\right) \tag{4.44}$$

which stays finite in the large R limit only for $\alpha > 1$. In this case, the $1/l^{\alpha-1}$ term dominates over the $1/l^\alpha$ term in 4.41, resulting in the estimate (by saddle point approximation after converting the l sum into an integral)

$$\rho_o(t)_{S\to\infty} \sim e^{-c'\, t^{1/\alpha}} \,, \tag{4.45}$$

the so-called stretched exponential or Kohlrausch law.

Hence, we find a very satisfying result. Our *ansatz* 4.35, which was motivated by causality constraints in the near-horizon geometry, is exactly the critical ultrametric landscape in which the thermodynamic limit becomes impossible. Indeed, for $\alpha = 1$ the exponents in 4.41 all diverge logarithmically as $S \to \infty$ and the random walk is completely spread up to infinity at any time $t > 0$.

The behavior of the autocorrelation function $\rho_o(t)$ is usually characterized in terms of the *spectral dimension*, $\tilde{d}$ defined in general in terms of the long-time behavior as

$$\rho_o(t) \sim t^{-\tilde{d}/2} \, . \tag{4.46}$$

With this definition, the Kohlrausch law 4.45 has an effectively infinite spectral dimension at late times, a behaviour that is characteristic of fast scramblers and diffusion in expander graphs in general.

Finally, the ballistic properties of the fast scrambler can be codified in terms of 4.45 as well, since the number of points covered by the distribution in time t is proportional to $1/\rho_o(t)$. The ultrametric radius of this 'ball' is thus

$$r_{eff}(t) \sim \log\left(1/\rho_o(t)\right) \sim t^{1/\alpha} \, . \tag{4.47}$$

Therefore, we recover the expected ballistic behaviour $r_{eff}(t) \sim t$ precisely in the limit $\alpha \to 1$.

Chapter 5

Summary

In this thesis we have advanced on several issues concerning the Fast Scrambling Conjecture [5] [6]. Our results are in support of this conjecture. In this last chapter, we will quickly review the main concepts and results of this thesis.

The heuristic arguments justifying the conjecture have been shown to depend crucially on one geometrical aspect common to every thermal horizon: the free fall time to the SH. This time scale is of the same order of the conjectured time scale, from we conclude that Fast Scramblers should evolve *ballistically*. In chapter 2, we study this geometrical aspect for generic types of Black Branes, resulting in numerous insights. For one, Fast Scramblers must be *small*, in the sense that their thermal length must be bigger than any of the other spatial length scales involved in the system. When the opposite is true, the free fall time just depends on the effective entropy contained in a single thermal cell. Thus Fast Scrambling only occurs within the thermal cell, a fact highlighted in [6]. On the other hand, in the specific case of the Super-Yang-Mill gauge theory in four dimensions defined on a torus, when considering phase transitions, or *topological flops*, interpolating from one regime to the other, we derive the effective theory of a single thermal cell. This theory is the Matrix Model of [21].

Secondly, within the phenomenological approach to the scrambling time, the *probe approximation*, we show that hyperbolic spaces, in their continuum and discrete versions, are natural Fast Scramblers. In this vein, we proceed to attack the Fast Scrambling time scale on these spaces from more fundamental perspectives, with two different out-

comes. The first one appears when the original definition, concerning the so-called *Page test*, is applied to these hyperbolic models. The conclusion is that finding *extensive* scalings of entanglement entropy should not be considered as a definite sign of Fast Scrambling. Exact computations of entanglement entropy are necessary. As this is a difficult task, we try to find other characterizations of Fast Scrambling. One possibility are the causality constraints of the model, or *signalling*, as was termed in [34]. Consistent with previous intuitions, we find that perturbations of Field Theories in Hyperbolic spaces in the thermal ensemble propagate *ballistically*.

The core of the thesis stems from the observation that the phase space and the dynamics of the near horizon region of every thermal horizon can be naturally described in the conformally related *optical* frame. This *optical* frame turns out to be, universally at the near horizon region, a hyperbolic space times the time line. The vacuum, or Hartle-Hawking state, is seen as a thermal state in this hyperboloid. Moreover, the specific technicalities of the conformal mapping allows for a definition of the SH. In the optical frame, the irrelevant couplings are position dependent, and diverge as we approach the horizon, calling for an ultraviolet completion of the theory. This naturally *defines* the concept of Λ-*stretched* horizon as the crossover from weak coupling to strong coupling dynamics. This crossover depends on the specific LEFT considered. When $\Lambda \sim M_p$, we recover the usual, weakly-coupled near horizon region, cut-off by a *Planckian* SH.

Lastly, all the previous observations are joined to construct three different models of information scrambling on event horizons. In the case that the Λ-*stretched* horizon covers the whole near horizon region, i.e we have a putative black hole dual to a weakly coupled CFT, expander graph or hyperbolic diffusion in the strong coupling region provides the right scrambling time scale. In the other case, when we have a weakly coupled near horizon region, we show how surface scattering effects on the Planckian SH convert the thermal atmosphere into an effective hyperbolic billiard, a classical example of hard chaos, which, in turn, highlights the expected chaotic nature of Black Holes and Matrix Models. In this case, the scrambling time scale is seen as the Liapunov time of the chaotic billiard: the time needed for erasure of any initially locally codified information. These two models, at first sight, do not provide us with any information about the dynamics

of the Planckian SH, a recurrent problem in Black Hole Physics. Using the Fast Scrambling Conjecture as a guide through these dynamics and the previous results concerning the flight times across the thermal atmosphere, we naturally propose a theory for information diffusion on this surface. This theory possesses an Ultrametric structure, a fact that can be traced back to the hyperbolic nature of the optical metric. Furthermore, the theory has very specific transition rates saturating stability bounds, a fact that can be traced back to the flight times through the thermal atmosphere, or the *optical depth*. This model, with these transition rates, is also a Fast Scrambler.

Further work is needed to confirm that some, or all of these structures appear in the dual Matrix Model description of Black Holes.

Appendix A

Completely Connected Physical Systems

The results concerning Fast Scrambling behaviour during the thesis may be considered *bulk* results. Therefore it is still lacking a proper understanding from the dual Matrix Models. Studies of these models have been carried out in [57, 58] numerically, and analytical results are obtained in [34]. In this section we advance some speculative considerations about this problem. We take a different route, trying to see if some of the *Fast Scrambling* structures uncovered during the thesis *emerge* under some approximation in the dual, completely connected, Matrix Models.

When considering physical models in which every degree of freedom interacts with every other degree of freedom, the first problem to arise when directly applying the standard diffusion method is that the scrambling time is of $\mathcal{O}(1)$, in appropriate units. Basically, diffusion takes place in one step. This is easily seen when considering a Random Walk in a graph that is completely connected. In this case, the second eigenvalue of the Adjacency Matrix tends to zero in the thermodynamic limit. If the probe particle has the same probability to go anywhere on the graph, its position is completely uncertain just after one step. This result remains unchanged when using a random stochastic matrix as the Adjacency Matrix.

The analogue in the quantum framework is a quantum state undergoing Random Unitary evolution. This kind of problem was studied in [59] and in [60], from which we inferred that scrambling is achieved

in one step. This is a natural occurrence. Applying a random unitary to a specific state should result in a pure random state. Due to the *Page* result, this is seen to be a scrambled state

At first, these results appear to violate the conjecture, but this is not the case when taking a closer look at the original statement [6]. A crucial condition in the conjecture is that the Hamiltonian should contain terms involving no more than $\mathcal{O}(1)$ degrees of freedom, in the large N limit. This is indeed what differentiates the evolution governed by the Matrix Theory Hamiltonian [21] from that of a Random evolution taken from the Circular Unitary ensemble. The latter is completely random, mixing in one step one particle states with $\mathcal{O}(N)$ particle states. In contrast, the Matrix Theory Hamiltonian, although completely non-local in *position* space, does not achieve this *quantum* non-locality, and only mixes one particle states with $\mathcal{O}(1)$ particle states in one step. This might imply that after one step, the perturbation has achieved only $\mathcal{O}(1)$-body entanglement.

Translating these heuristic arguments to more rigorous mathematical statements is part of our on-going work. For now, we will construct a classical model which emulates these ideas and demonstrates how scrambling is achieved after $\log N$ steps, even in a completely connected model.

The core observation challenging the diffusion approach of the scrambling time is that the attainment of equilibrium by the probability distribution does not imply that the random walk has visited $\mathcal{O}(N)$ vertices.

For example, after the diffusion time has elapsed, in flat graphs models or expander graphs, the random walk has visited $\mathcal{O}(n^{d/2})$ or $\mathcal{O}(\log n)$ respectively [1]. In this way, the random walk has not explored $\mathcal{O}(N)$ vertices, as would be required to scramble the whole system.

Consequently, we define the following process. We begin with a random walk, representing the first perturbation of the system. When the random walk arrives to a vertex, another random walk is created (i.e, at each time step we double the number of random walks). This represents how degrees of freedom become messengers of an original perturbation once another messenger has interacted with them. A natural quantity to study would be the time scale in which we have probability of $\mathcal{O}(1)$for having visited $\mathcal{O}(n)$ vertices.

[1]The number of vertices visited cannot exceed the number of steps taken

We could not arrive to a proper Markov process formulation of these dynamics. In particular it is not simply characterized by a random walk with a certain regular adjacency matrix in some bigger configuration space. However, the question we are seeking does not need a rigorous formulation.

First, we notice that the number of random walks populating the graph is exactly 2^t, where t is a discrete time variable. So, by construction, we immediately get a lower bound for the diffusion time of this branching process on any type of graphs.

$$2^t \simeq n \longrightarrow t \simeq \log n \tag{A.1}$$

Interestingly enough, we see that complete graphs do not achieve equilibrium for this process in one step. We will study this process for these types of graphs more precisely below. Let us first consider this process for the more common flat and expander cases.

After $\log n$ steps we have created n random walks. For an expander graph, in the worst case, we have to wait $\mathcal{O}(\log n)$ steps so that each of all those n Random Walks become uniform over the graph. When this occurs, we have $\mathcal{O}(n)$ Random Walks randomly distributed over $\mathcal{O}(n)$ sites, and therefore the probability of having visited $\mathcal{O}(n)$ different sites is of $\mathcal{O}(1)$. In this way, we again conclude that expanders are good examples of Fast Scramblers.

In the flat case, the situation is quite different. One might assume that enlarging the number of Random Walks would decrease the diffusion time, but this is not the case. As every Random Walk is created by the arrival of another Random Walk to that specific site, the time for this Branching process is still of $\mathcal{O}(n^{\frac{2}{d}})$ because the time of traversing the system remains unchanged.

The time scales for these two types of graphs do not change. It might seem that we have created some unjustified and unneeded interpretations of the information processing through these systems. The most striking case occurs when we observe a complete graph. We are going to study this case in detail now.

We draw the process in Figure A.1. We observe that the branching process creates a perfect *tree* with probability 1 in the large N limit. The term *tree* means that no vertex is visited twice. The actual relationship between these *time trees* and the trees founded in the bulk

description of Black Holes is unclear and probably misleading. In any case, it is a possibility worth exploring.

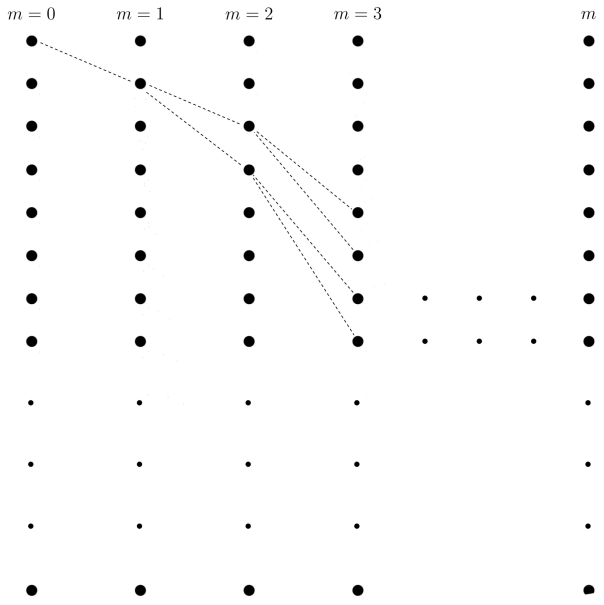

Figure A.1: In this picture it is shown a Branching Markov process in a completely connected model. The number of random Walks is duplicated at each time step. In the limit in which the number of nodes $N \to \infty$ the probability of no repetition and the subsequent formation of a *time tree* is equal to one, until times of $\mathcal{O}(\log N)$.

To check this *tree emergence*, we may just compute the probability by counting the number of trees at each time step and dividing it by the total number of possibilities. In particular, after m steps the total number of possible configurations is given by

$$\Omega = n^{2^0} \times n^{2^1} \times n^{2^2} \times \cdots \times n^{2^{m-1}} = n^{\sum_{i=0}^{i=m-1} 2^i} = n^{2^m - 1} \tag{A.2}$$

On the other hand, the total number of *trees* is seen to be

$$\begin{aligned}\Omega_{\rm tree} &= (n-1)\times(n-2)(n-1)\times(n-1)(n-1)(n-1)(n-1)\times\cdots\times \\ &\times[n-(\sum_{i=0}^{i=m-2}2^i+1)][n-(\sum_{i=0}^{i=m-2}2^i+1)-1]\times\cdots\times \\ &\times[n-(\sum_{i=0}^{i=m-1}2^i+1)] \end{aligned} \tag{A.3}$$

Ordering term by term, the probability of creating a tree *randomly* is given by

$$\begin{aligned}\frac{\Omega_{\rm tree}}{\Omega} &= \frac{(n-1)(n-2)\cdots(n-(2^m-1))}{n^{2^m-1}} = \\ &\frac{(n-1)}{n}\times\frac{(n-1)(n-2)}{n^2}\times\cdots\times \\ &\times\frac{(n-2^{m-1})(n-2^{m-1}-1)\cdots\times(n-(2^m-1))}{n^{2^{m-1}}}\end{aligned} \tag{A.4}$$

So that

$$\frac{\Omega_{\rm tree}}{\Omega} = P_1\times P_2\times\cdots P_m \tag{A.5}$$

with

$$(1-\frac{2^m-1}{n})^{2^{m-1}} < P_m < (1-\frac{2^{m-1}}{n})^{2^{m-1}} \tag{A.6}$$

Taking now $m = a\log(n)+1$ it is easy to show that

$$\lim_{n\to\infty} P_m = 1 \Longleftrightarrow 0 \le a < 1/2 \tag{A.7}$$

and

$$\lim_{n\to\infty} P_m = 0 \Longleftrightarrow 1/2 \le a \le 1 \tag{A.8}$$

In other words, during times of $\mathcal{O}(\log(n))$, the process creates these *time trees* with probability 1.

There are two speculative directions worth exploring. For one, the simple model may represent the flow of information in completely

connected models. The Fast Scrambling Conjecture would follow naturally by the *tree* construction.

A second possibility is that the bulk description of the Black Hole geometrically represents this flow of Information. If this were the case, this simple toy-model would help us understand why the space time picture breaks at the SH. In this model, the *dynamically generated* geometric description breaks down with probability 1 after times of $\mathcal{O}(\log(n))$. This, in the bulk description, is exactly the location of the Planckian SH.

The computation done in this section, concerning the *tree* probability, supposes that the perturbations propagating through the sites, *the probes*, are distinguishable. We also studied the case in which these perturbations are undistinguishable. The result turned out to be the same to the one described above.

Bibliography

[1] Jose L.F. Barbon and Javier M. Magan. Chaotic Fast Scrambling At Black Holes. *Phys.Rev.*, D84:106012, 2011.

[2] Jose L.F. Barbon and Javier M. Magan. Fast Scramblers Of Small Size. *JHEP*, 1110:035, 2011.

[3] Jose L.F. Barbon and Javier M. Magan. Fast Scramblers, Horizons and Expander Graphs. *JHEP*, 1208:016, 2012.

[4] Jose L.F. Barbon and Javier M. Magan. Fast Scramblers And Ultrametric Blcak Holes Horizons.

[5] Patrick Hayden and John Preskill. Black holes as mirrors: Quantum information in random subsystems. *JHEP*, 0709:120, 2007.

[6] Yasuhiro Sekino and Leonard Susskind. Fast Scramblers. *JHEP*, 0810:065, 2008.

[7] Leonard Susskind. Addendum to Fast Scramblers. 2011.

[8] Jacob D. Bekenstein. Black Holes and entropy. *Physical Review D*, 7:23332346, 1973.

[9] Stephen W. hawking. Particle creation by black holes. *Communications in Mathematical Physics*, 43:199–220, 1974.

[10] Ofer Aharony and Tom Banks. Note on the quantum mechanics of M theory. *JHEP*, 9903:016, 1999.

[11] G.W. Gibbons and M.J. Perry. Black Holes and thermal green funcitons. *Proc. R. Soc. Lond. A*, 358:467–494, 1978.

[12] Gerard 't Hooft. Dimensional reduction in quantum gravity. 1993.

[13] Leonard Susskind. The World as a hologram. *J.Math.Phys.*, 36:6377–6396, 1995.

[14] Juan Martin Maldacena. The Large N limit of superconformal field theories and supergravity. *Adv.Theor.Math.Phys.*, 2:231–252, 1998.

[15] Ofer Aharony, Steven S. Gubser, Juan Martin Maldacena, Hirosi Ooguri, and Yaron Oz. Large N field theories, string theory and gravity. *Phys.Rept.*, 323:183–386, 2000.

[16] Thibaut Damour. Black-hole eddy currents. *Phys. Rev. D*, 18:3598–3604, Nov 1978.

[17] K. S. Thorne, R. H. Price, and D. A. MacDonald. *Black holes: The membrane paradigm*. 1986.

[18] Leonard Susskind and James Lindesay. *An Introduction To Black Holes, Information And The String Theory Revolution: The Holographic Universe*. World Scientific Publishing Company, 2004.

[19] Leonard Susskind, Larus Thorlacius, and John Uglum. The Stretched horizon and black hole complementarity. *Phys.Rev.*, D48:3743–3761, 1993.

[20] Ahmed Almheiri, Donald Marolf, Joseph Polchinski, and James Sully. Black Holes: Complementarity or Firewalls? *JHEP*, 1302:062, 2013.

[21] Tom Banks, W. Fischler, S.H. Shenker, and Leonard Susskind. M theory as a matrix model: A Conjecture. *Phys.Rev.*, D55:5112–5128, 1997.

[22] Daniel Harlow and Patrick Hayden. Quantum Computation vs. Firewalls. 2013.

[23] Christoph Dankert, Richard Cleve, Joseph Emerson, and Etera Livine. Exact and Approximate Unitary 2-design: Constructions and Applications. *Phys.Rev.*, 2009.

[24] Nissan Itzhaki, Juan Martin Maldacena, Jacob Sonnenschein, and Shimon Yankielowicz. Supergravity and the large N limit of theories with sixteen supercharges. *Phys.Rev.*, D58:046004, 1998.

[25] Shinsei Ryu and Tadashi Takayanagi. Holographic derivation of entanglement entropy from AdS/CFT. *Phys.Rev.Lett.*, 96:181602, 2006.

[26] Shinsei Ryu and Tadashi Takayanagi. Aspects of Holographic Entanglement Entropy. *JHEP*, 0608:045, 2006.

[27] Tatsuma Nishioka, Shinsei Ryu, and Tadashi Takayanagi. Holographic Entanglement Entropy: An Overview. *J.Phys.*, A42:504008, 2009.

[28] Jose L.F. Barbon and Carlos A. Fuertes. Holographic entanglement entropy probes (non)locality. *JHEP*, 0804:096, 2008.

[29] J.L.F. Barbon and E. Rabinovici. Extensivity versus holography in anti-de Sitter spaces. *Nucl.Phys.*, B545:371–384, 1999.

[30] J.L.F. Barbon, I.I. Kogan, and E. Rabinovici. On stringy thresholds in SYM / AdS thermodynamics. *Nucl.Phys.*, B544:104–144, 1999.

[31] J.L.F. Barbon and E. Rabinovici. On 1/N corrections to the entropy of noncommutative Yang-Mills theories. *JHEP*, 9912:017, 1999.

[32] R. Gregory and R. Laflamme. Black strings and p-branes are unstable. *Phys.Rev.Lett.*, 70:2837–2840, 1993.

[33] Ruth Gregory and Raymond Laflamme. The Instability of charged black strings and p-branes. *Nucl.Phys.*, B428:399–434, 1994.

[34] Nima Lashkari, Douglas Stanford, Matthew Hastings, Tobias Osborne, and Patrick Hayden. Towards the Fast Scrambling Conjecture. *JHEP*, 1304:022, 2013.

[35] Don N. Page. Average entropy of a subsystem. *Phys.Rev.Lett.*, 71:1291–1294, 1993.

[36] H. J. Carmichael. *An open systems approach to quantum optics.* UniversitLibre de Bruxelles, 1991.

[37] R. Feynman and F. Vernon. The theory of a general quantum system interacting with a linear dissipative system. *Annals of Physics*, 24:118–173, October 1963.

[38] A. O. Caldeira and A. J. Leggett. Path integral approach to quantum Brownian motion. *Physica A Statistical Mechanics and its Applications*, 121:587–616, September 1983.

[39] Wojciech Hubert Zurek. *Rev. Mod. Phys.*, (3):715–775, May.

[40] John Preskill. Lectures on quantum computation.

[41] Elliott H. Lieb and Derek W. Robinson. The finite group velocity of quantum spin systems. *Communications in Mathematical Physics*, 28(3):251–257, September 1972.

[42] Shlomo Hoory, Nathan Linial, Avi Wigderson, and An Overview. Expander graphs and their applications. *Bull. Amer. Math. Soc. (N.S*, 43:439–561, 2006.

[43] Alexander Lubotzky. Expander Graphs in Pure and Applied Mathematics. May 2011.

[44] Ccile Monthus and Christophe Texier. Random walk on the bethe lattice and hyperbolic brownian motion. *Journal of Physics A: Mathematical and General*, 29(10):2399, 1996.

[45] M. Hein, W. Dür, J. Eisert, R. Raussendorf, M. Van den Nest, and H. J. Briegel. Entanglement in Graph States and its Applications, February 2006.

[46] G.W. Gibbons and C.M. Warnick. Universal properties of the near-horizon optical geometry. *Phys.Rev.*, D79:064031, 2009.

[47] P. Candelas and J.S. Dowker. FIELD THEORIES ON CONFORMALLY RELATED SPACE-TIMES: SOME GLOBAL CONSIDERATIONS. *Phys.Rev.*, D19:2902, 1979.

[48] Horacio Casini, Marina Huerta, and Robert C. Myers. Towards a derivation of holographic entanglement entropy. *JHEP*, 1105:036, 2011.

[49] J.J Bisognano and E.H. Wichmann. On the Duality Condition for Quantum Fields. *J.Math.Phys.*, 17:303–321, 1976.

[50] J.J Bisognano and E.H. Wichmann. On the Duality Condition for a Hermitian Scalar Field. *J.Math.Phys.*, 16:985–1007, 1975.

[51] Ivo Sachs and Sergey N. Solodukhin. Horizon holography. *Phys.Rev.*, D64:124023, 2001.

[52] Gerard 't Hooft. On the Quantum Structure of a Black Hole. *Nucl.Phys.*, B256:727, 1985.

[53] J.L.F. Barbon. Horizon divergences of fields and strings in black hole backgrounds. *Phys.Rev.*, D50:2712–2718, 1994.

[54] Martin C. Gutzwiller. *Chaos in Classical and Quantum Mechanics*. Number 1 in Interdisciplinary Applied Mathematics. Springer-Verlag, New York, NY, 1990.

[55] N. L. Balazs and A. Voros. Chaos on the pseudosphere. , 143:109–240, November 1986.

[56] Andrew T. Ogielski and D. L. Stein. Dynamics on ultrametric spaces. *Phys. Rev. Lett.*, 55:1634–1637, Oct 1985.

[57] Curtis Asplund, David Berenstein, and Diego Trancanelli. Evidence for fast thermalization in the plane-wave matrix model. *Phys.Rev.Lett.*, 107:171602, 2011.

[58] Curtis T. Asplund, David Berenstein, and Eric Dzienkowski. Large N classical dynamics of holographic matrix models. *Phys.Rev.*, D87:084044, 2013.

[59] Vinayak and Marko Znidaric. Subsystem dynamics under random hamiltonian evolution. 2011.

[60] M. B. Hastings. Random Unitaries Give Quantum Expanders, June 2007.